mathematics

MDPI

Article

Global Stability of a Reaction–Diffusion Malaria/COVID-19 Coinfection Dynamics Model

Ahmed M. Elaiw [1,*] and Afnan D. Al Agha [2]

[1] Department of Mathematics, Faculty of Science, King Abdulaziz University, P.O. Box 80203, Jeddah 21589, Saudi Arabia
[2] Department of Mathematical Science, College of Engineering, University of Business and Technology, Jeddah 21361, Saudi Arabia
* Correspondence: aelaiwksu.edu.sa@kau.edu.sa

Abstract: Severe acute respiratory syndrome coronavirus 2 (SARS-CoV-2) is a new virus which infects the respiratory system and causes the coronavirus disease 2019 (COVID-19). The coinfection between malaria and COVID-19 has been registered in many countries. This has risen an urgent need to understand the dynamics of coinfection. In this paper, we construct a reaction–diffusion in-host malaria/COVID-19 model. The model includes seven-dimensional partial differential equations that explore the interactions between seven compartments, healthy red blood cells (RBCs), infected RBCs, free merozoites, healthy epithelial cells (ECs), infected ECs, free SARS-CoV-2 particles, and antibodies. The biological validation of the model is confirmed by establishing the nonnegativity and boundedness of the model's solutions. All equilibrium points with the corresponding existence conditions are calculated. The global stability of all equilibria is proved by picking up appropriate Lyapunov functionals. Numerical simulations are used to enhance and visualize the theoretical results. We found that the equilibrium points show the different cases when malaria and SARS-CoV-2 infections occur as mono-infection or coinfection. The shared antibody immune response decreases the concentrations of SARS-CoV-2 and malaria merozoites. This can have an important role in reducing the severity of SARS-CoV-2 if the immune response works effectively.

Keywords: SARS-CoV-2; COVID-19; malaria; immune response; diffusion; global stability

MSC: 35B35; 37N25; 92B05

check for updates

Citation: Elaiw, A.M.; Al Agha, A.D. Global Stability of a Reaction–Diffusion Malaria/COVID-19 Coinfection Dynamics Model. *Mathematics* **2022**, *10*, 4390. https://doi.org/10.3390/math10224390

Academic Editor: Carla M.A. Pinto

Received: 18 October 2022
Accepted: 17 November 2022
Published: 21 November 2022

Publisher's Note: MDPI stays neutral with regard to jurisdictional claims in published maps and institutional affiliations.

Copyright: © 2022 by the authors. Licensee MDPI, Basel, Switzerland. This article is an open access article distributed under the terms and conditions of the Creative Commons Attribution (CC BY) license (https://creativecommons.org/licenses/by/4.0/).

1. Introduction

The coronavirus disease 2019 (COVID-19) is a viral disease that appeared in China at the end of 2019 and spread to most countries of the world. The severe acute respiratory syndrome coronavirus 2 (SARS-CoV-2) is the cause of COVID-19. Malaria-endemic regions face a great challenge due to the possibility of coinfection between malaria and other viral diseases. Indeed, malaria/COVID-19 coinfection has been founded in several countries [1]. This has increased the necessity to understand the dynamics of the coinfection and its effect on the patient.

SARS-CoV-2 is an RNA virus and belongs to the family Coronaviridae [2]. It uses the angiotensin-converting enzyme 2 (ACE2) receptor to step into the ECs [3]. Such receptor is expressed in kidney, heart, gastrointestinal tract, blood vessels, and other organs [4]. The human-to-human transmission of SARS-CoV-2 occurs via respiratory droplets containing viruses [5]. Eleven vaccines for COVID-19 were approved by the World Health Organization (WHO) for emergency use. These include Novavax/Nuvaxovid, Bharat Biotech/Covaxin, CanSino/Convidecia, Pfizer/BioNTech/Comirnaty, Moderna/Spikevax, Serum Institute of India COVOVAX (Novavax formulation), Janssen (Johnson & Johnson)/Jcovden, Oxford/AstraZeneca/Vaxzevria, Serum Institute of India Covishield (Oxford/AstraZeneca formulation), Sinopharm (Beijing)/Covilo, and Sinovac/CoronaVac [6].

There are a number of other effective vaccines that are not yet approved by the WHO. On 22 October 2020, the U.S. Food and Drug Administration (FDA) approved the antiviral drug Veklury (remdesivir) for the treatment of COVID-19 cases who need hospitalization [7]. It is utilized for adults and pediatric patients 12 years of age and older (with weight $\geq$ 40 kg) [7].

On the other hand, malaria is a parasitic disease attributable to Plasmodium parasites [5,8]. There are five types of Plasmodium parasites: P. malariae, P. knowlesi, P. vivax, P. falciparum, and P. ovale . However, P. falciparum is the deadliest malaria parasite. Infected Anopheles mosquitoes transmit the malaria parasite to humans [8]. There are two stages for malaria infection in the body: the liver stage and the blood stage [8]. The blood stage is responsible for most of the clinical symptoms. At the blood stage, the parasites, in the form of a merozoite attack, infect the red blood cells (RBCs) [8]. After rupturing a cell, 8–32 daughter merozoites are produced [8]. Preventive chemotherapies are utilized to treat malaria infection and their consequences [9]. In this paper, we focus on the blood stage of malaria infection.

Malaria and COVID-19 have common symptoms including fever, headache, fatigue, myalgia and difficulty in breathing [10–12]. This can cause difficulty in the clinical diagnosis of malaria and SARS-CoV-2 coinfection [4,5]. Wrong or late diagnosis of coinfection can have a bad effect on the health of the patient [13]. The incubation periods for Plasmodium falciparum malaria and SARS-CoV-2 are 7–14 days and 2–17 days, respectively, and this enhances the possibility of coinfection [5,13]. In fact, malaria/COVID-19 coinfection has been found in several countries [13–15]. Some studies indicated that the coinfection could increase the severity of SARS-CoV-2 infection [1,13]. Wilairatana et al. [1] presented a review article and identified studies of malaria/COVID-19 coinfection and compared them from several aspects including: the possible correlations between COVID-19 and malaria, the prevalence of malaria infection among COVID-19 patients, the risk of oxidative stress in the malaria/COVID-19 coinfection, the role of sex in the malaria/COVID-19 coinfection, the effect of malaria coinfection on the clearance of SARS-CoV-2 in COVID-19 patients, the clinical severity of COVID-19, treatment of COVID-19, mean duration of the hospitalized and the underlying comorbidities. Hussein et al. [16] reported that coinfection with malaria and COVID-19 is associated with increased all-cause in-hospital mortality compared to a single-infection with SARS-CoV2. Nevertheless, several studies mentioned that the neutralizing antibodies against Plasmodium falciparum can also be effective against SARS-CoV-2 particles. This can minimize the severity of SARS-CoV-2 infection in coinfected patients [4,17–19]. Thus, understanding the dynamics of coinfection is very crucial in order to find better ways to deal with and treat this group of patients.

Mathematical modeling is considered as one of the most substantial tools that is used to support medical studies during epidemics. Malaria models at the blood stage have been explored in many works (see for example [20–26]). In addition, many COVID-19 models have been formulated and studied. These models can be classified into epidemiological models and in-host models. Epidemiological models study the transmission of COVID-19 between individuals (see for example [27–32]). On the other hand, in-host models study the interactions between SARS-CoV-2 and cells inside the body (see for example [33–38]). In fact, in-host models have received less attention than between-host models. In a recent work [39], the malaria/SARS-CoV-2 coinfection model has been developed and investigated. All the above-mentioned models assume that parasites, viruses, and cells are distributed homogeneously in the body. However, this assumption is not realistic in biological systems as the diffusion of particles causes spatial variations within the body. Considering spatial diffusion converts the ODE model into a PDE model, which allows the compartments to vary in space and time. This will give a more accurate description of the model's dynamics. Therefore, some malaria models (see for example [8,40]) and SARS-CoV-2 models (see for example [39,41]) are formulated using partial differential equations (PDEs) to take into account the diffusion of some components in the model. Actually, the coinfection of COVID-19 with malaria is an active area of research. Current studies are trying to deeply understand the dynamics of this coinfection. This will help to effectively treat coinfected patients and

save their lives. Mathematical modeling can support these studies and reduce the number of experiments needed to test hypotheses. We noted that a diffusive malaria/COVID-19 coinfection model has not yet been considered. In this paper, we formulate a reaction–diffusion malaria/COVID-19 model. This model considers the interactions between healthy RBCs, infected RBCs, free merozoites, healthy ECs, infected ECs, free SARS-CoV-2 particles, and antibodies. For this model, we (i) validate the boundedness and nonnegativity of solutions, (ii) calculate all model's equilibria and extract the conditions of their existence, (iii) show the global stability of equilibria, and (iv) enhance the analytical results by executing some numerical simulations.

The paper is written as follows: Section 2 gives a description for the proposed model. Section 3 shows the properties of the model's solutions. Furthermore, it calculates all models' equilibria. Section 4 introduces the Lyapunov method to establish the global stability of all model's equilibria. Section 5 is devoted for numerical simulations. Finally, the results are discussed and some future research points are suggested in Section 6.

2. Reaction–Diffusion Malaria/COVID-19 Model with Immune Response

In this section, we give a detailed description of the proposed model. We construct the malaria/COVID-19 coinfection model as a system of seven PDEs:

$$\begin{cases} \frac{\partial U(x,t)}{\partial t} = D_U \Delta U(x,t) + \sigma_1 - \beta_m U(x,t) M(x,t) - d_1 U(x,t), \\ \frac{\partial I(x,t)}{\partial t} = D_I \Delta I(x,t) + \beta_m U(x,t) M(x,t) - d_2 I(x,t), \\ \frac{\partial M(x,t)}{\partial t} = D_M \Delta M(x,t) + \eta d_2 I(x,t) - q_1 M(x,t) Z(x,t) - d_3 M(x,t), \\ \frac{\partial Y(x,t)}{\partial t} = D_Y \Delta Y(x,t) + \sigma_2 - \beta_v Y(x,t) V(x,t) - d_4 Y(x,t), \\ \frac{\partial N(x,t)}{\partial t} = D_N \Delta N(x,t) + \beta_v Y(x,t) V(x,t) - d_5 N(x,t), \\ \frac{\partial V(x,t)}{\partial t} = D_V \Delta V(x,t) + eN(x,t) - q_2 V(x,t) Z(x,t) - d_6 V(x,t), \\ \frac{\partial Z(x,t)}{\partial t} = D_Z \Delta Z(x,t) + p_1 M(x,t) Z(x,t) + p_2 V(x,t) Z(x,t) - d_7 Z(x,t), \end{cases} \tag{1}$$

for $t > 0$ and $x \in \Gamma$, where $U(x,t)$, $I(x,t)$, $M(x,t)$, $Y(x,t)$, $N(x,t)$, $V(x,t)$, and $Z(x,t)$ stand for the concentrations of healthy RBCs, infected RBCs, free merozoites, healthy ECs, infected ECs, free SARS-CoV-2 particles, and antibodies. Healthy RBCs are generated at a constant rate σ_1, get infected by merozoites at rate $\beta_m UM$, and die at rate $d_1 U$. Infected RBCs die at rate $d_2 I$ and burst to generate η merozoites per infected cell. Free merozoites die at rate $d_3 M$ and are cleared by antibodies at rate $q_1 MZ$. Healthy ECs are recruited from its source at rate σ_2, get infected by SARS-CoV-2 at rate $\beta_v YV$ and die at rate $d_4 Y$. Infected ECs die at rate $d_5 N$ and release SARS-CoV-2 at rate eN. SARS-CoV-2 particles are eliminated by antibodies at rate $q_2 VZ$ and die at rate $d_6 V$. Antibodies die at a natural death rate $d_7 Z$ and are stimulated to target malaria merozoites and SARS-CoV-2 at rates $p_1 MZ$ and $p_2 VZ$, respectively. The spatial domain Γ is continuous, bounded and its boundary $\partial\Gamma$ is smooth. $\Delta = \frac{\partial^2}{\partial x^2}$ is the Laplacian operator. We assume that each component $C(x,t)$ of the model diffused in the domain with a diffusion coefficient D_C. The initial conditions (ICs) of model (1) are defined as the following:

$$\begin{array}{llll} U(x,0) = \gamma_1(x), & I(x,0) = \gamma_2(x), & M(x,0) = \gamma_3(x), & Y(x,0) = \gamma_4(x), \\ N(x,0) = \gamma_5(x), & V(x,0) = \gamma_6(x), & Z(x,0) = \gamma_7(x), & \gamma_i(x),\ i = 1,2,\ldots,7,\ x \in \bar{\Gamma}. \end{array} \tag{2}$$

The boundary conditions are given by the following Neumann boundary conditions (NBCs):

$$\frac{\partial U}{\partial \vec{v}} = \frac{\partial I}{\partial \vec{v}} = \frac{\partial M}{\partial \vec{v}} = \frac{\partial Y}{\partial \vec{v}} = \frac{\partial N}{\partial \vec{v}} = \frac{\partial V}{\partial \vec{v}} = \frac{\partial Z}{\partial \vec{v}} = 0, \quad t > 0, \quad x \in \partial\Gamma, \tag{3}$$

where $\frac{\partial}{\partial \vec{v}}$ is the outward normal derivative on $\partial\Gamma$. This type of boundary condition simulates a natural barrier that prevents cells and viruses from crossing the boundary.

3. Properties of Solutions

In this section, we verify the basic properties of model (1) including the existence, nonnegativity, and boundedness of the solutions. Furthermore, we evaluate all possible equilibrium points with their conditions of existence.

Let $\mathbb{H} = \mathbb{C}_b(\bar{\Gamma}, \mathbb{R}^7)$ be the set of all bounded and continuous functions from $\bar{\Gamma}$ to $\mathbb{R}^7$, and $\mathbb{H}_+ = \mathbb{C}_b(\bar{\Gamma}, \mathbb{R}^7_+) \subset \mathbb{H}$. The positive cone $\mathbb{H}_+$ induces a partial order on $\mathbb{H}$. Let $\|\phi\|_{\mathbb{H}} = \sup_{x\in\bar{\Gamma}} |\phi(x)|$, where $|\cdot|$ is the Euclidean norm on $\mathbb{R}^7$. This reveals that $(\mathbb{H}, \|\cdot\|_{\mathbb{H}})$ is a Banach lattice [42,43].

Theorem 1. *Assume that $D_U = D_I$, $D_Y = D_N$, and $D_M = D_V = D_Z$. Then, model (1) has a unique, nonnegative and bounded solution defined on $\bar{\Gamma} \times [0, +\infty)$ for any initial conditions satisfying (2).*

Proof. For any $\gamma = (\gamma_1, \gamma_2, \gamma_3, \gamma_4, \gamma_5, \gamma_6, \gamma_7)^T \in \mathbb{H}_+$, we define $A = (A_1, A_2, A_3, A_4, A_5, A_6, A_7)^T : \mathbb{H}_+ \to \mathbb{H}$ by

$$\begin{cases} A_1(\gamma)(x) = \sigma_1 - \beta_m \gamma_1(x)\gamma_3(x) - d_1\gamma_1(x), \\ A_2(\gamma)(x) = \beta_m \gamma_1(x)\gamma_3(x) - d_2\gamma_2(x), \\ A_3(\gamma)(x) = \eta d_2\gamma_2(x) - q_1\gamma_3(x)\gamma_7(x) - d_3\gamma_3(x), \\ A_4(\gamma)(x) = \sigma_2 - \beta_v \gamma_4(x)\gamma_6(x) - d_4\gamma_4(x), \\ A_5(\gamma)(x) = \beta_v \gamma_4(x)\gamma_6(x) - d_5\gamma_5(x), \\ A_6(\gamma)(x) = e\gamma_5(x) - q_2\gamma_6(x)\gamma_7(x) - d_6\gamma_6(x), \\ A_7(\gamma)(x) = p_1\gamma_3(x)\gamma_7(x) + p_2\gamma_6(x)\gamma_7(x) - d_7\gamma_7(x). \end{cases}$$

We note that A is locally Lipschitz on $\mathbb{H}_+$. We rewrite system (1)–(3) as the abstract differential equation

$$\begin{cases} \frac{dQ}{dt} = DQ + A(Q), \ t > 0, \\ Q_0 = \gamma \in \mathbb{H}_+, \end{cases}$$

where $Q = (U, I, M, Y, N, V, Z)^T$ and $DQ = (D_U\Delta U, D_I\Delta I, D_M\Delta M, D_Y\Delta Y, D_N\Delta N, D_V\Delta V, 4D_Z\Delta Z)^T$. It is possible to show that

$$\lim_{h\to 0^+} \frac{1}{h} \operatorname{dist}(\gamma + hA(\gamma), \mathbb{H}_+) = 0, \ \gamma \in \mathbb{H}_+.$$

According to [42–44], systems (1)–(3) have a unique nonnegative mild solution on $[0, T_x)$, which is the maximal existence time interval. Next, we show that the solutions of model (1) are bounded. We define

$$\Theta_1(x,t) = U(x,t) + I(x,t).$$

Since $D_U = D_I$, we obtain that

$$\begin{aligned} \frac{\partial \Theta_1(x,t)}{\partial t} - D_U\Delta\Theta_1(x,t) &= \sigma_1 - d_1U(x,t) - d_2I(x,t) \\ &\leq \sigma_1 - \zeta_1[U(x,t) + I(x,t)] \\ &= \sigma_1 - \zeta_1\Theta_1(x,t), \end{aligned}$$

where $\zeta_1 = \min\{d_1, d_2\}$. Thus, $\Theta_1(x,t)$ satisfies the following system:

$$\begin{cases} \dfrac{\partial \Theta_1(x,t)}{\partial t} - D_U \Delta \Theta_1(x,t) \leq \sigma_1 - \zeta_1 \Theta_1(x,t), \\ \dfrac{\partial \Theta_1}{\partial \vec{v}} = 0, \\ \Theta_1(x,0) = \gamma_1(x) + \gamma_2(x) \geq 0. \end{cases}$$

Let $\widetilde{\Theta}_1(t)$ be a solution to the following ODE

$$\begin{cases} \dfrac{d\widetilde{\Theta}_1(t)}{dt} = \sigma_1 - \zeta_1 \widetilde{\Theta}_1(t), \\ \widetilde{\Theta}_1(0) = \max\limits_{x \in \bar{\Gamma}} \Theta_1(x,0). \end{cases}$$

Thus, $\widetilde{\Theta}_1(t) \leq \max\left\{ \dfrac{\sigma_1}{\zeta_1}, \max\limits_{x \in \bar{\Gamma}} \Theta_1(x,0) \right\}$. Comparison principle [45] provides that $\Theta_1(x,t) \leq \widetilde{\Theta}_1(t)$. Therefore, we have

$$\Theta_1(x,t) \leq \max\left\{ \frac{\sigma_1}{\zeta_1}, \max_{x \in \bar{\Gamma}} \Theta_1(x,0) \right\} := \kappa_1.$$

Accordingly, $U(x,t)$ and $I(x,t)$ are bounded. Let

$$\Theta_2(x,t) = Y(x,t) + N(x,t).$$

As $D_Y = D_N$, we obtain

$$\begin{aligned} \frac{\partial \Theta_2(x,t)}{\partial t} - D_Y \Delta \Theta_2(x,t) =& \sigma_2 - d_4 Y(x,t) - d_5 N(x,t) \\ \leq& \sigma_2 - \zeta_2 [Y(x,t) + N(x,t)] \\ =& \sigma_2 - \zeta_2 \Theta_2(x,t), \end{aligned}$$

where $\zeta_2 = \min\{d_4, d_5\}$. Comparison principle [45] implies that

$$\Theta_2(x,t) \leq \max\left\{ \frac{\sigma_2}{\zeta_2}, \max_{x \in \bar{\Gamma}} \Theta_2(x,0) \right\} := \kappa_2.$$

This proves the boundedness of $Y(x,t)$ and $N(x,t)$. Finally, we define a function

$$\Theta_3(x,t) = M(x,t) + \frac{q_1 p_2}{p_1 q_2} V(x,t) + \frac{q_1}{p_1} Z(x,t).$$

Since $D_M = D_V = D_Z$, $I(x,t) \leq \kappa_1$, and $N(x,t) \leq \kappa_2$, we have

$$\begin{aligned} \frac{\partial \Theta_3(x,t)}{\partial t} - D_M \Delta \Theta_3(x,t) =& \eta d_2 I(x,t) + \frac{e q_1 p_2}{p_1 q_2} N(x,t) - d_3 M(x,t) - \frac{q_1 p_2 d_6}{p_1 q_2} V(x,t) - \frac{q_1 d_7}{p_1} Z(x,t) \\ \leq& \eta d_2 \kappa_1 + \frac{e q_1 p_2}{p_1 q_2} \kappa_2 - \zeta_3 \left[M(x,t) + \frac{q_1 p_2}{p_1 q_2} V(x,t) + \frac{q_1}{p_1} Z(x,t) \right] \\ =& \eta d_2 \kappa_1 + \frac{e q_1 p_2}{p_1 q_2} \kappa_2 - \zeta_3 \Theta_3(x,t), \end{aligned}$$

where $\zeta_3 = \min\{d_3, d_6, d_7\}$. Based on the comparison principle [45], we obtain

$$\Theta_3(x,t) \leq \max\left\{ \frac{\eta d_2 \kappa_1}{\zeta_3} + \frac{e q_1 p_2 \kappa_2}{p_1 q_2 \zeta_3}, \max_{x \in \bar{\Gamma}} \Theta_3(x,0) \right\}.$$

Thus, $M(x,t)$, $V(x,t)$, and $Z(x,t)$ are bounded. Consequently, all solutions are bounded on $[0, T_x)$. Based on the standard theory for semi-linear parabolic systems [46], the solutions are bounded on $\bar{\Gamma} \times [0, +\infty)$. □

Proposition 1. *There exist positive parameters $\mathcal{R}_{0m}$, $\mathcal{R}_{1m}$, $\mathcal{R}_p$ $\mathcal{R}_{0v}$, and $\mathcal{R}_{1v}$ such that model (1) admits seven equilibria as:*

(1) The uninfected equilibrium E_0 always exists;
(2) The SARS-CoV-2-free equilibrium without immune response E_1 exists if $\mathcal{R}_{0m} > 1$;
(3) The SARS-CoV-2-free equilibrium E_2 exists if $\mathcal{R}_{1m} > 1$;
(4) The malaria-free equilibrium without immune response E_3 exists if $\mathcal{R}_{0v} > 1$;
(5) The malaria-free equilibrium E_4 exists if $\mathcal{R}_{1v} > 1$;
(6) The malaria/COVID-19 coinfection immune-free equilibrium E_5 exists if $\mathcal{R}_{0m} > 1$ and $\mathcal{R}_{0v} > 1$;
(7) The malaria/COVID-19 coinfection equilibrium E_6 exists if $\mathcal{R}_p > 1 + \frac{\eta\beta_m\sigma_1 p_1 q_2}{q_1 d_6(p_1 d_1 + \beta_m d_7)}$, $\mathcal{R}_{0m} + \frac{q_1 d_6}{q_2 d_3} > 1 + \frac{e\beta_v q_1 \sigma_2 p_2}{q_2 d_3 d_5(p_2 d_4 + \beta_v d_7)}$, and $\mathcal{R}_{0m} + \frac{e\beta_m \sigma_2 p_2}{p_1 d_1 d_5 d_6} > 1 + \frac{\beta_m(p_2 d_4 + \beta_v d_7)}{\beta_v p_1 d_1}$.

Proof. Each equilibrium of system (1) satisfies the following algebraic system:

$$\begin{cases} 0 = \sigma_1 - \beta_m UM - d_1 U, \\ 0 = \beta_m UM - d_2 I, \\ 0 = \eta d_2 I - q_1 MZ - d_3 M, \\ 0 = \sigma_2 - \beta_v YV - d_4 Y, \\ 0 = \beta_v YV - d_5 N, \\ 0 = eN - q_2 VZ - d_6 V, \\ 0 = p_1 MZ + p_2 VZ - d_7 Z. \end{cases} \tag{4}$$

By solving (4), we obtain the following equilibria:

(1) The uninfected equilibrium $E_0 = (U_0, 0, 0, Y_0, 0, 0, 0)$, where

$$U_0 = \frac{\sigma_1}{d_1} > 0, \quad Y_0 = \frac{\sigma_2}{d_4} > 0.$$

Thus, the equilibrium E_0 always exists.

(2) The malaria single-infection without immunity equilibrium is given by $E_1 = (U_1, I_1, M_1, Y_1, 0, 0, 0)$, where

$$U_1 = \frac{d_3}{\eta\beta_m}, \quad I_1 = \frac{d_1 d_3}{\eta\beta_m d_2}(\mathcal{R}_{0m} - 1), \quad M_1 = \frac{d_1}{\beta_m}(\mathcal{R}_{0m} - 1), \quad Y_1 = \frac{\sigma_2}{d_4},$$

where $\mathcal{R}_{0m} = \frac{\eta\beta_m\sigma_1}{d_1 d_3}$. We note that U_1 and Y_1 are positive, while I_1 and M_1 are positive for $\mathcal{R}_{0m} > 1$. Thus, E_1 exists when $\mathcal{R}_{0m} > 1$. Here, $\mathcal{R}_{0m}$ is a threshold parameter, which specifies the establishment of malaria infection.

(3) The malaria single-infection with immunity equilibrium $E_2 = (U_2, I_2, M_2, Y_2, 0, 0, Z_2)$. The components are given by

$$U_2 = \frac{\sigma_1 p_1}{p_1 d_1 + \beta_m d_7}, \quad I_2 = \frac{\beta_m \sigma_1 d_7}{d_2(p_1 d_1 + \beta_m d_7)}, \quad M_2 = \frac{d_7}{p_1}, \quad Y_2 = \frac{\sigma_2}{d_4}, \quad Z_2 = \frac{d_3}{q_1}(\mathcal{R}_{1m} - 1),$$

where $\mathcal{R}_{1m} = \frac{\eta\beta_m\sigma_1 p_1}{d_3(p_1 d_1 + \beta_m d_7)}$. We see that U_2, I_2, M_2 and Y_2 are always positive, while $Z_2 > 0$ when $\mathcal{R}_{1m} > 1$. Therefore, E_2 exists if $\mathcal{R}_{1m} > 1$. $\mathcal{R}_{1m}$ is a threshold

parameter which sets the initiation of antibody immune response against malaria merozoites.

(4) The SARS-CoV-2 single-infection without immunity equilibrium is defined as $E_3 = (U_3, 0, 0, Y_3, N_3, V_3, 0)$. The components are given by

$$U_3 = \frac{\sigma_1}{d_1}, \quad Y_3 = \frac{d_5 d_6}{e\beta_v}, \quad N_3 = \frac{d_4 d_6}{e\beta_v}(\mathcal{R}_{0v} - 1), \quad V_3 = \frac{d_4}{\beta_v}(\mathcal{R}_{0v} - 1),$$

where $\mathcal{R}_{0v} = \dfrac{e\beta_v \sigma_2}{d_4 d_5 d_6}$. Notably, U_3 and Y_3 are always positive, while N_3 and V_3 are positive when $\mathcal{R}_{0v} > 1$. Here, $\mathcal{R}_{0v}$ is a threshold parameter which determines the establishment of SARS-CoV-2 infection.

(5) The SARS-CoV-2 single-infection with immunity is given by $E_4 = (U_4, 0, 0, Y_4, N_4, V_4, Z_4)$, where

$$U_4 = \frac{\sigma_1}{d_1}, \quad Y_4 = \frac{\sigma_2 p_2}{p_2 d_4 + \beta_v d_7}, \quad N_4 = \frac{\beta_v \sigma_2 d_7}{d_5(p_2 d_4 + \beta_v d_7)}, \quad V_4 = \frac{d_7}{p_2}, \quad Z_4 = \frac{d_6}{q_2}(\mathcal{R}_{1v} - 1),$$

where $\mathcal{R}_{1v} = \dfrac{e\beta_v \sigma_2 p_2}{d_5 d_6 (p_2 d_4 + \beta_v d_7)}$. We see that U_4, Y_4, N_4 and V_4 are always positive, while $Z_4 > 0$ if $\mathcal{R}_{1v} > 1$. Hence, E_4 exists if $\mathcal{R}_{1v} > 1$. The threshold parameter $\mathcal{R}_{1v}$ marks the establishment of antibody immunity against SARS-CoV-2 infection.

(6) The malaria/SARS-CoV-2 coinfection without immunity equilibrium is given by $E_5 = (U_5, I_5, M_5, Y_5, N_5, V_5, 0)$, where

$$U_5 = \frac{d_3}{\eta\beta_m}, \quad I_5 = \frac{d_1 d_3}{\eta\beta_m d_2}(\mathcal{R}_{0m} - 1), \quad M_5 = \frac{d_1}{\beta_m}(\mathcal{R}_{0m} - 1),$$
$$Y_5 = \frac{d_5 d_6}{e\beta_v}, \quad N_5 = \frac{d_4 d_6}{e\beta_v}(\mathcal{R}_{0v} - 1), \quad V_5 = \frac{d_4}{\beta_v}(\mathcal{R}_{0v} - 1).$$

The components U_5 and Y_5 are always positive. I_5 and M_5 are positive when $\mathcal{R}_{0m} > 1$, while N_5 and V_5 are positive when $\mathcal{R}_{0v} > 1$. Consequently, E_5 exists when $\mathcal{R}_{0m} > 1$ and $\mathcal{R}_{0v} > 1$.

(7) The malaria/SARS-CoV-2 coinfection with immunity equilibrium is given by $E_6 = (U_6, I_6, M_6, Y_6, N_6, V_6, Z_6)$, where

$$U_6 = \frac{\sigma_1 p_1}{p_1 d_1 + \beta_m(d_7 - p_2 V_6)}, \quad I_6 = \frac{\sigma_1 \beta_m (d_7 - p_2 V_6)}{d_2[p_1 d_1 + \beta_m(d_7 - p_2 V_6)]}, \quad M_6 = \frac{d_7 - p_2 V_6}{p_1},$$
$$Y_6 = \frac{q_2 d_3 d_5 (p_1 d_1 + \beta_m d_7)(\mathcal{R}_{1m} - 1) + \beta_m p_2 q_2 d_3 d_5 V_6 + d_5 q_1 d_6 [p_1 d_1 + \beta_m (d_7 - p_2 V_6)]}{e q_1 \beta_v [p_1 d_1 + \beta_m (d_7 - p_2 V_6)]},$$
$$N_6 = \frac{q_2 d_3 (p_1 d_1 + \beta_m d_7)(\mathcal{R}_{1m} - 1) + \beta_m p_2 q_2 d_3 V_6 + q_1 d_6 [p_1 d_1 + \beta_m (d_7 - p_2 V_6)]}{e q_1 [p_1 d_1 + \beta_m (d_7 - p_2 V_6)]} V_6,$$
$$Z_6 = \frac{d_3 (p_1 d_1 + \beta_m d_7)(\mathcal{R}_{1m} - 1) + \beta_m p_2 d_3 V_6}{q_1 [p_1 d_1 + \beta_m (d_7 - p_2 V_6)]}.$$

By substituting Y_6 in the fourth equation of model (1), we obtain

$$e\beta_v q_1 \sigma_2 [p_1 d_1 + \beta_m (d_7 - p_2 V_6)] - d_4 d_5 [p_1 d_1 + \beta_m (d_7 - p_2 V_6)][q_1 d_6 - q_2 d_3] - \eta\beta_m \sigma_1 p_1 q_2 d_4 d_5$$
$$- \beta_v d_5 V_6 [p_1 d_1 + \beta_m (d_7 - p_2 V_6)](q_1 d_6 - q_2 d_3) - \eta\beta_m \beta_v \sigma_1 p_1 q_2 d_5 V_6 = 0.$$

Thus, V_6 fulfills the following equation

$$\beta_m\beta_v p_2 d_5(q_1 d_6 - q_2 d_3){V_6}^2 + \Big(\beta_m q_1 p_2 d_4 d_5 d_6 + \beta_v p_1 d_1 q_2 d_3 d_5 + \beta_m\beta_v q_2 d_3 d_5 d_7 - e\beta_m\beta_v q_1\sigma_2 p_2$$
$$- \beta_m p_2 q_2 d_3 d_4 d_5 - \beta_v p_1 q_1 d_1 d_5 d_6 - \beta_m\beta_v q_1 d_5 d_6 d_7 - \eta\beta_m\beta_v\sigma_1 p_1 q_2 d_5\Big) V_6 + e\beta_v p_1 q_1 d_1\sigma_2$$
$$+ e\beta_m\beta_v q_1\sigma_2 d_7 + p_1 d_1 q_2 d_3 d_4 d_5 + \beta_m q_2 d_3 d_4 d_5 d_7 - p_1 d_1 q_1 d_4 d_5 d_6 - \beta_m q_1 d_4 d_5 d_6 d_7 - \eta\beta_m\sigma_1 p_1 q_2 d_4 d_5 = 0.$$

Let us define a function $G(V)$ as follows:

$$G(V) = aV^2 + bV + c,$$

where

$$\begin{aligned}
a =& \beta_m\beta_v p_2 d_5(q_1 d_6 - q_2 d_3),\\
b =& \beta_m q_1 p_2 d_4 d_5 d_6 + \beta_v p_1 d_1 q_2 d_3 d_5 + \beta_m\beta_v q_2 d_3 d_5 d_7 - e\beta_m\beta_v q_1\sigma_2 p_2 - \beta_m p_2 q_2 d_3 d_4 d_5\\
& - \beta_v p_1 q_1 d_1 d_5 d_6 - \beta_m\beta_v q_1 d_5 d_6 d_7 - \eta\beta_m\beta_v\sigma_1 p_1 q_2 d_5,\\
c =& e\beta_v p_1 q_1 d_1\sigma_2 + e\beta_m\beta_v q_1\sigma_2 d_7 + p_1 d_1 q_2 d_3 d_4 d_5 + \beta_m q_2 d_3 d_4 d_5 d_7 - p_1 d_1 q_1 d_4 d_5 d_6\\
& - \beta_m q_1 d_4 d_5 d_6 d_7 - \eta\beta_m\sigma_1 p_1 q_2 d_4 d_5.
\end{aligned}$$

By computing the value of $G(V)$ at $V = 0$, we obtain

$$\begin{aligned}
G(0) =& e\beta_v q_1\sigma_2(p_1 d_1 + \beta_m d_7) + q_2 d_3 d_4 d_5(p_1 d_1 + \beta_m d_7) - q_1 d_4 d_5 d_6(p_1 d_1 + \beta_m d_7) - \eta\beta_m\sigma_1 p_1 q_2 d_4 d_5\\
=& q_1 d_4 d_5 d_6(p_1 d_1 + \beta_m d_7)\left[\frac{e\beta_v q_1\sigma_2 + q_2 d_3 d_4 d_5}{q_1 d_4 d_5 d_6} - 1 - \frac{\eta\beta_m\sigma_1 p_1 q_2}{q_1 d_6(p_1 d_1 + \beta_m d_7)}\right]\\
=& q_1 d_4 d_5 d_6(p_1 d_1 + \beta_m d_7)\left[\mathcal{R}_p - 1 - \frac{\eta\beta_m\sigma_1 p_1 q_2}{q_1 d_6(p_1 d_1 + \beta_m d_7)}\right],
\end{aligned}$$

where $\mathcal{R}_p = \dfrac{e\beta_v q_1\sigma_2 + q_2 d_3 d_4 d_5}{q_1 d_4 d_5 d_6}$. We note that $G(0) > 0$ if

$$\mathcal{R}_p > 1 + \frac{\eta\beta_m\sigma_1 p_1 q_2}{q_1 d_6(p_1 d_1 + \beta_m d_7)}. \tag{5}$$

In addition, we find that

$$\begin{aligned}
G\left(\frac{d_7}{p_2}\right) =& \frac{-1}{p_2}\left[\eta\beta_m\sigma_1 p_1 q_2 d_5(p_2 d_4 + \beta_v d_7) + p_1 q_1 d_1 d_5 d_6(p_2 d_4 + \beta_v d_7) - p_1 d_1 q_2 d_3 d_5(p_2 d_4 + \beta_v d_7) - e\beta_v p_1 q_1 d_1\sigma_2 p_2\right]\\
=& -\frac{p_1 d_1 q_2 d_3 d_5(p_2 d_4 + \beta_v d_7)}{p_2}\left[\mathcal{R}_{0m} + \frac{q_1 d_6}{q_2 d_3} - 1 - \frac{e\beta_v q_1\sigma_2 p_2}{q_2 d_3 d_5(p_2 d_4 + \beta_v d_7)}\right]
\end{aligned}$$

Thus, $G\left(\dfrac{d_7}{p_2}\right) < 0$ if

$$\mathcal{R}_{0m} + \frac{q_1 d_6}{q_2 d_3} > 1 + \frac{q_1 d_6}{q_2 d_3}\mathcal{R}_{1v}. \tag{6}$$

This implies that there exists a root $0 < V^* < \dfrac{d_7}{p_2}$ such that $G(V^*) = 0$. Let $V_6 = V^*$ and observe that for $0 < V_6 < \dfrac{d_7}{p_2}$ and $\mathcal{R}_{1m} > 1$ ($\mathcal{R}_{1m} > 1$ is naturally satisfied at E_6 because E_2 coexists with E_6 when $\mathcal{R}_{1m} > 1$, but it will not be stable as can be concluded from Theorem 4), we have $U_6 > 0$, $I_6 > 0$, $M_6 > 0$, $Y_6 > 0$, $N_6 > 0$ and $Z_6 > 0$. Similarly, to find the third existence condition of E_6, we form a function of Z and extract the conditions at which there is a positive root. This will give

$$\mathcal{R}_{0m} + \frac{e\beta_m\sigma_2 p_2}{p_1 d_1 d_5 d_6} > 1 + \frac{\beta_m(p_2 d_4 + \beta_v d_7)}{\beta_v p_1 d_1}. \tag{7}$$

It follows that E_6 exists if conditions (5), (6), and (7) are met. □

4. Global Stability of Equilibria

This section confirms the global stability of all equilibrium points by building appropriate Lyapunov functionals. Define a Lyapunov functional

$$\Delta_i(t) = \int_\Gamma \widetilde{\Delta}_i(x,t)\,\mathrm{d}x,$$

and let K_i' be the largest invariant subset of $K_i = \left\{(U,I,M,Y,N,V,Z) \mid \frac{d\Delta_i}{dt} = 0\right\}$, $i = 0,1,\ldots,6$.

Theorem 2. *The uninfected equilibrium E_0 is globally asymptotically stable (GAS) when $\mathcal{R}_{0m} \le 1$ and $\mathcal{R}_{0v} \le 1$.*

Proof. Define

$$\widetilde{\Delta}_0(x,t) = U_0\left(\frac{U}{U_0} - 1 - \ln\frac{U}{U_0}\right) + I + \frac{1}{\eta}M + \frac{eq_1p_2}{\eta p_1q_2d_5}Y_0\left(\frac{Y}{Y_0} - 1 - \ln\frac{Y}{Y_0}\right) + \frac{eq_1p_2}{\eta p_1q_2d_5}N + \frac{q_1p_2}{\eta p_1q_2}V + \frac{q_1}{\eta p_1}Z.$$

Then, we have

$$\begin{aligned}
\frac{\partial\widetilde{\Delta}_0}{\partial t} =& \left(1 - \frac{U_0}{U}\right)\left(D_U\Delta U + \sigma_1 - \beta_m UM - d_1U\right) + D_I\Delta I + \beta_m UM - d_2I \\
&+ \frac{1}{\eta}\left(D_M\Delta M + \eta d_2I - q_1MZ - d_3M\right) + \frac{eq_1p_2}{\eta p_1q_2d_5}\left(1 - \frac{Y_0}{Y}\right)\left(D_Y\Delta Y + \sigma_2 - \beta_vYV - d_4Y\right) \\
&+ \frac{eq_1p_2}{\eta p_1q_2d_5}\left(D_N\Delta N + \beta_vYV - d_5N\right) + \frac{q_1p_2}{\eta p_1q_2}\left(D_V\Delta V + eN - q_2VZ - d_6V\right) \\
&+ \frac{q_1}{\eta p_1}\left(D_Z\Delta Z + p_1MZ + p_2VZ - d_7Z\right) \\
=& \left(1 - \frac{U_0}{U}\right)\left(\sigma_1 - d_1U\right) + \frac{eq_1p_2}{\eta p_1q_2d_5}\left(1 - \frac{Y_0}{Y}\right)\left(\sigma_2 - d_4Y\right) + \left(\beta_mU_0 - \frac{d_3}{\eta}\right)M \\
&+ \left(\frac{eq_1p_2\beta_v}{\eta p_1q_2d_5}Y_0 - \frac{q_1p_2d_6}{\eta p_1q_2}\right)V - \frac{q_1d_7}{\eta p_1}Z + \left(1 - \frac{U_0}{U}\right)D_U\Delta U + D_I\Delta I + \frac{1}{\eta}D_M\Delta M \\
&+ \frac{eq_1p_2}{\eta p_1q_2d_5}\left(1 - \frac{Y_0}{Y}\right)D_Y\Delta Y + \frac{eq_1p_2}{\eta p_1q_2d_5}D_N\Delta N + \frac{q_1p_2}{\eta p_1q_2}D_V\Delta V + \frac{q_1}{\eta p_1}D_Z\Delta Z.
\end{aligned}$$

By calculating the time derivative of $\Delta_0(t)$, we have

$$\begin{aligned}
\frac{d\Delta_0}{dt} =& -d_1\int_\Gamma \frac{(U-U_0)^2}{U}\,\mathrm{d}x - \frac{eq_1p_2d_4}{\eta p_1q_2d_5}\int_\Gamma \frac{(Y-Y_0)^2}{Y}\,\mathrm{d}x + \frac{d_3}{\eta}(\mathcal{R}_{0m}-1)\int_\Gamma M\,\mathrm{d}x \\
&+ \frac{q_1p_2d_6}{\eta p_1q_2}(\mathcal{R}_{0v}-1)\int_\Gamma V\,\mathrm{d}x - \frac{q_1d_7}{\eta p_1}\int_\Gamma Z\,\mathrm{d}x + D_U\int_\Gamma\left(1 - \frac{U_0}{U}\right)\Delta U\,\mathrm{d}x + D_I\int_\Gamma \Delta I\,\mathrm{d}x \\
&+ \frac{1}{\eta}D_M\int_\Gamma \Delta M\,\mathrm{d}x + \frac{eq_1p_2}{\eta p_1q_2d_5}D_Y\int_\Gamma\left(1 - \frac{Y_0}{Y}\right)\Delta Y\,\mathrm{d}x + \frac{eq_1p_2}{\eta p_1q_2d_5}D_N\int_\Gamma \Delta N\,\mathrm{d}x \\
&+ \frac{q_1p_2}{\eta p_1q_2}D_V\int_\Gamma \Delta V\,\mathrm{d}x + \frac{q_1}{\eta p_1}D_Z\int_\Gamma \Delta Z\,\mathrm{d}x. \qquad (8)
\end{aligned}$$

Depending on the Divergence theorem and NBCs, we have

$$\begin{aligned}
0 &= \int_{\partial\Gamma}\nabla\chi\cdot\vec{v}\,\mathrm{d}x = \int_\Gamma \mathrm{div}(\nabla\chi)\,\mathrm{d}x = \int_\Gamma \Delta\chi\,\mathrm{d}x, \\
0 &= \int_{\partial\Gamma}\frac{1}{\chi}\nabla\chi\cdot\vec{v}\,\mathrm{d}x = \int_\Gamma \mathrm{div}(\frac{1}{\chi}\nabla\chi)\,\mathrm{d}x = \int_\Gamma\left[\frac{\Delta\chi}{\chi} - \frac{\|\nabla\chi\|^2}{\chi^2}\right]\mathrm{d}x, \quad \text{for } \chi \in \{U,I,M,Y,N,V,Z\}.
\end{aligned}$$

This implies that

$$\begin{aligned}&\int_\Gamma \Delta\chi \,\mathrm{d}x = 0,\\ &\int_\Gamma \frac{\Delta\chi}{\chi}\,\mathrm{d}x = \int_\Gamma \frac{\|\nabla\chi\|^2}{\chi^2}\,\mathrm{d}x, \quad \text{for} \quad \chi \in \{U, I, M, Y, N, V, Z\}.\end{aligned} \tag{9}$$

By applying (9) to (8), we obtain

$$\begin{aligned}\frac{d\Delta_0}{dt} =& -d_1\int_\Gamma \frac{(U-U_0)^2}{U}\,\mathrm{d}x - \frac{eq_1p_2d_4}{\eta p_1q_2d_5}\int_\Gamma \frac{(Y-Y_0)^2}{Y}\,\mathrm{d}x + \frac{d_3}{\eta}(\mathcal{R}_{0m}-1)\int_\Gamma M\,\mathrm{d}x\\ &+ \frac{q_1p_2d_6}{\eta p_1q_2}(\mathcal{R}_{0v}-1)\int_\Gamma V\,\mathrm{d}x - \frac{q_1d_7}{\eta p_1}\int_\Gamma Z\,\mathrm{d}x - D_UU_0\int_\Gamma \frac{\|\nabla U\|^2}{U^2}\,\mathrm{d}x - \frac{eq_1p_2}{\eta p_1q_2d_5}D_YY_0\int_\Gamma \frac{\|\nabla Y\|^2}{Y^2}\,\mathrm{d}x.\end{aligned}$$

We note that $\frac{d\Delta_0}{dt} \le 0$ when $\mathcal{R}_{0m} \le 1$ and $\mathcal{R}_{0v} \le 1$. In addition, $\frac{d\Delta_0}{dt} = 0$ when $U = U_0$, $Y = Y_0$, and $M = V = Z = 0$. The solutions tend to $K_0^{'}$ which contains elements with $M = V = 0$ and then $\frac{dM}{dt} = 0$ and $\frac{dV}{dt} = 0$. The third and sixth equations of system (1) imply that $I = N = 0$. Then, $K_0^{'} = \{E_0\}$ and thus LaSalle's invariance principle (LIP) [47] assures the global asymptotic stability of E_0 when $\mathcal{R}_{0m} \le 1$ and $\mathcal{R}_{0v} \le 1$. □

Theorem 3. *Assume that $\mathcal{R}_{0m} > 1$. Then, the malaria single-infection without immunity equilibrium E_1 is GAS if $\mathcal{R}_{0v} \le 1$ and $\mathcal{R}_{1m} \le 1$.*

Proof. Define

$$\begin{aligned}\widetilde{\Delta}_1(x,t) =& U_1\left(\frac{U}{U_1} - 1 - \ln\frac{U}{U_1}\right) + I_1\left(\frac{I}{I_1} - 1 - \ln\frac{I}{I_1}\right) + \frac{1}{\eta}M_1\left(\frac{M}{M_1} - 1 - \ln\frac{M}{M_1}\right)\\ &+ \frac{eq_1p_2}{\eta p_1q_2d_5}Y_1\left(\frac{Y}{Y_1} - 1 - \ln\frac{Y}{Y_1}\right) + \frac{eq_1p_2}{\eta p_1q_2d_5}N + \frac{q_1p_2}{\eta p_1q_2}V + \frac{q_1}{\eta p_1}Z.\end{aligned}$$

Then, we obtain

$$\begin{aligned}\frac{\partial\widetilde{\Delta}_1}{\partial t} =& \left(1 - \frac{U_1}{U}\right)\left(D_U\Delta U + \sigma_1 - \beta_mUM - d_1U\right) + \left(1 - \frac{I_1}{I}\right)\left(D_I\Delta I + \beta_mUM - d_2I\right)\\ &+ \frac{1}{\eta}\left(1 - \frac{M_1}{M}\right)\left(D_M\Delta M + \eta d_2I - q_1MZ - d_3M\right) + \frac{eq_1p_2}{\eta p_1q_2d_5}\left(1 - \frac{Y_1}{Y}\right)\left(D_Y\Delta Y + \sigma_2 - \beta_vYV - d_4Y\right)\\ &+ \frac{eq_1p_2}{\eta p_1q_2d_5}\left(D_N\Delta N + \beta_vYV - d_5N\right) + \frac{q_1p_2}{\eta p_1q_2}\left(D_V\Delta V + eN - q_2VZ - d_6V\right)\\ &+ \frac{q_1}{\eta p_1}\left(D_Z\Delta Z + p_1MZ + p_2VZ - d_7Z\right).\end{aligned} \tag{10}$$

The equilibrium conditions at E_1 are

$$\begin{cases}\sigma_1 = \beta_mU_1M_1 + d_1U_1,\\ \beta_mU_1M_1 = d_2I_1,\\ d_2I_1 = \dfrac{d_3}{\eta}M_1,\\ \sigma_2 = d_4Y_1.\end{cases} \tag{11}$$

By utilizing (11) to collect terms of Equation (10), we obtain

$$\begin{aligned}\frac{\partial\widetilde{\Delta}_1}{\partial t} =&\left(1-\frac{U_1}{U}\right)\left(d_1U_1-d_1U\right)+3\beta_mU_1M_1-\beta_mU_1M_1\frac{U_1}{U}-\beta_mU_1M_1\frac{UI_1M}{U_1IM_1}\\&+\frac{eq_1p_2}{\eta p_1q_2d_5}\left(1-\frac{Y_1}{Y}\right)\left(d_4Y_1-d_4Y\right)-\beta_mU_1M_1\frac{IM_1}{I_1M}+\left(\frac{eq_1p_2\beta_v}{\eta p_1q_2d_5}Y_1-\frac{q_1p_2d_6}{\eta p_1q_2}\right)V\\&+\left(\frac{q_1}{\eta}M_1-\frac{q_1d_7}{\eta p_1}\right)Z+\left(1-\frac{U_1}{U}\right)D_U\Delta U+\left(1-\frac{I_1}{I}\right)D_I\Delta I+\frac{1}{\eta}\left(1-\frac{M_1}{M}\right)D_M\Delta M\\&+\frac{eq_1p_2}{\eta p_1q_2d_5}\left(1-\frac{Y_1}{Y}\right)D_Y\Delta Y+\frac{eq_1p_2}{\eta p_1q_2d_5}D_N\Delta N+\frac{q_1p_2}{\eta p_1q_2}D_V\Delta V+\frac{q_1}{\eta p_1}D_Z\Delta Z.\end{aligned}$$

By computing $\frac{d\Delta_1}{dt}$, we obtain

$$\begin{aligned}\frac{d\Delta_1}{dt} =&-d_1\int_\Gamma\frac{(U-U_1)^2}{U}\,\mathrm{d}x-\frac{eq_1p_2d_4}{\eta p_1q_2d_5}\int_\Gamma\frac{(Y-Y_1)^2}{Y}\,\mathrm{d}x+\beta_mU_1M_1\int_\Gamma\left(3-\frac{U_1}{U}-\frac{IM_1}{I_1M}-\frac{UI_1M}{U_1IM_1}\right)\mathrm{d}x\\&+\frac{q_1p_2d_6}{\eta p_1q_2}(\mathcal{R}_{0v}-1)\int_\Gamma V\,\mathrm{d}x+\frac{q_1(p_1d_1+\beta_md_7)}{\eta p_1\beta_m}(\mathcal{R}_{1m}-1)\int_\Gamma Z\,\mathrm{d}x+D_U\int_\Gamma\left(1-\frac{U_1}{U}\right)\Delta U\,\mathrm{d}x\\&+D_I\int_\Gamma\left(1-\frac{I_1}{I}\right)\Delta I\,\mathrm{d}x+\frac{1}{\eta}D_M\int_\Gamma\left(1-\frac{M_1}{M}\right)\Delta M\,\mathrm{d}x+\frac{eq_1p_2}{\eta p_1q_2d_5}D_Y\int_\Gamma\left(1-\frac{Y_1}{Y}\right)\Delta Y\,\mathrm{d}x\\&+\frac{eq_1p_2}{\eta p_1q_2d_5}D_N\int_\Gamma\Delta N\,\mathrm{d}x+\frac{q_1p_2}{\eta p_1q_2}D_V\int_\Gamma\Delta V\,\mathrm{d}x+\frac{q_1}{\eta p_1}D_Z\int_\Gamma\Delta Z\,\mathrm{d}x\\=&-d_1\int_\Gamma\frac{(U-U_1)^2}{U}\,\mathrm{d}x-\frac{eq_1p_2d_4}{\eta p_1q_2d_5}\int_\Gamma\frac{(Y-Y_1)^2}{Y}\,\mathrm{d}x+\beta_mU_1M_1\int_\Gamma\left(3-\frac{U_1}{U}-\frac{IM_1}{I_1M}-\frac{UI_1M}{U_1IM_1}\right)\mathrm{d}x\\&+\frac{q_1p_2d_6}{\eta p_1q_2}(\mathcal{R}_{0v}-1)\int_\Gamma V\,\mathrm{d}x+\frac{q_1(p_1d_1+\beta_md_7)}{\eta p_1\beta_m}(\mathcal{R}_{1m}-1)\int_\Gamma Z\,\mathrm{d}x-D_UU_1\int_\Gamma\frac{\|\nabla U\|^2}{U^2}\,\mathrm{d}x\\&-D_II_1\int_\Gamma\frac{\|\nabla I\|^2}{I^2}\,\mathrm{d}x-\frac{1}{\eta}D_MM_1\int_\Gamma\frac{\|\nabla M\|^2}{M^2}\,\mathrm{d}x-\frac{eq_1p_2}{\eta p_1q_2d_5}D_YY_1\int_\Gamma\frac{\|\nabla Y\|^2}{Y^2}\,\mathrm{d}x.\end{aligned}$$

Thus, we see that $\frac{d\Delta_1}{dt}\leq 0$ if $\mathcal{R}_{0v}\leq 1$ and $\mathcal{R}_{1m}\leq 1$. In addition, $\frac{d\Delta_1}{dt}=0$ when $U=U_1$, $I=I_1$, $M=M_1$, $Y=Y_1$, and $V=Z=0$. The solutions tend to $K_1^{'}$, which has $V=0$ and then $\frac{dV}{dt}=0$. From the sixth equation of (1), we obtain $N=0$. Hence, $K_1^{'}=\{E_1\}$. Accordingly, LIP proves the global asymptotic stability of E_1 if $\mathcal{R}_{0m}>1$, $\mathcal{R}_{0v}\leq 1$ and $\mathcal{R}_{1m}\leq 1$. □

Theorem 4. *Suppose that $\mathcal{R}_{1m}>1$. Then, the malaria single-infection with immunity equilibrium E_2 is GAS when $\mathcal{R}_p\leq 1+\frac{\eta\beta_m\sigma_1p_1q_2}{q_1d_6(p_1d_1+\beta_md_7)}$.*

Proof. Consider

$$\begin{aligned}\widetilde{\Delta}_2(x,t) =&U_2\left(\frac{U}{U_2}-1-\ln\frac{U}{U_2}\right)+I_2\left(\frac{I}{I_2}-1-\ln\frac{I}{I_2}\right)+\frac{1}{\eta}M_2\left(\frac{M}{M_2}-1-\ln\frac{M}{M_2}\right)+\frac{eq_1p_2}{\eta p_1q_2d_5}Y_2\left(\frac{Y}{Y_2}-1-\ln\frac{Y}{Y_2}\right)\\&+\frac{eq_1p_2}{\eta p_1q_2d_5}N+\frac{q_1p_2}{\eta p_1q_2}V+\frac{q_1}{\eta p_1}Z_2\left(\frac{Z}{Z_2}-1-\ln\frac{Z}{Z_2}\right).\end{aligned}$$

Then, we obtain

$$\begin{aligned}\frac{\partial\widetilde{\Delta}_2}{\partial t} =&\left(1-\frac{U_2}{U}\right)\left(D_U\Delta U+\sigma_1-\beta_m UM-d_1U\right)+\left(1-\frac{I_2}{I}\right)\left(D_I\Delta I+\beta_m UM-d_2I\right)\\&+\frac{1}{\eta}\left(1-\frac{M_2}{M}\right)\left(D_M\Delta M+\eta d_2I-q_1MZ-d_3M\right)+\frac{eq_1p_2}{\eta p_1q_2d_5}\left(1-\frac{Y_2}{Y}\right)\left(D_Y\Delta Y+\sigma_2-\beta_vYV-d_4Y\right)\\&+\frac{eq_1p_2}{\eta p_1q_2d_5}\left(D_N\Delta N+\beta_vYV-d_5N\right)+\frac{q_1p_2}{\eta p_1q_2}\left(D_V\Delta V+eN-q_2VZ-d_6V\right)\\&+\frac{q_1}{\eta p_1}\left(1-\frac{Z_2}{Z}\right)\left(D_Z\Delta Z+p_1MZ+p_2VZ-d_7Z\right).\end{aligned}\tag{12}$$

The equilibrium conditions at E_2 are computed as

$$\begin{cases}\sigma_1=\beta_mU_2M_2+d_1U_2,\\ \beta_mU_2M_2=d_2I_2,\\ d_2I_2=\dfrac{d_3}{\eta}M_2+\dfrac{q_1}{\eta}M_2Z_2,\\ \sigma_2=d_4Y_2,\\ \dfrac{q_1}{\eta}M_2Z_2=\dfrac{q_1d_7}{\eta p_1}Z_2.\end{cases}$$

After using the equilibrium conditions to collect terms of Equation (12), we obtain

$$\begin{aligned}\frac{\partial\widetilde{\Delta}_2}{\partial t} =&\left(1-\frac{U_2}{U}\right)\left(d_1U_2-d_1U\right)+\frac{eq_1p_2}{\eta p_1q_2d_5}\left(1-\frac{Y_2}{Y}\right)\left(d_4Y_2-d_4Y\right)+3\beta_mU_2M_2-\beta_mU_2M_2\frac{U_2}{U}\\&-\beta_mU_2M_2\frac{UI_2M}{U_2IM_2}-\beta_mU_2M_2\frac{IM_2}{I_2M}+\left(\frac{eq_1p_2\beta_v}{\eta p_1q_2d_5}Y_2-\frac{q_1p_2d_6}{\eta p_1q_2}-\frac{q_1p_2}{\eta p_1}Z_2\right)V+\left(1-\frac{U_2}{U}\right)D_U\Delta U\\&+\left(1-\frac{I_2}{I}\right)D_I\Delta I+\frac{1}{\eta}\left(1-\frac{M_2}{M}\right)D_M\Delta M+\frac{eq_1p_2}{\eta p_1q_2d_5}\left(1-\frac{Y_2}{Y}\right)D_Y\Delta Y+\frac{eq_1p_2}{\eta p_1q_2d_5}D_N\Delta N\\&+\frac{q_1p_2}{\eta p_1q_2}D_V\Delta V+\frac{q_1}{\eta p_1}\left(1-\frac{Z_2}{Z}\right)D_Z\Delta Z.\end{aligned}$$

By using the values of Y_2 and Z_2, we have

$$\begin{aligned}\frac{eq_1p_2\beta_v}{\eta p_1q_2d_5}Y_2-\frac{q_1p_2d_6}{\eta p_1q_2}-\frac{q_1p_2}{\eta p_1}Z_2=&\frac{e\beta_vq_1\sigma_2p_2}{\eta p_1q_2d_4d_5}-\frac{q_1p_2d_6}{\eta p_1q_2}-\frac{q_1p_2(\eta\beta_m\sigma_1p_1-p_1d_1d_3-\beta_md_3d_7)}{\eta p_1q_1(p_1d_1+\beta_md_7)}\\=&\frac{q_1p_2d_6}{\eta p_1q_2}\left[\frac{e\beta_vq_1\sigma_2+q_2d_3d_4d_5}{q_1d_4d_5d_6}-1-\frac{\eta\beta_m\sigma_1p_1q_2}{q_1d_6(p_1d_1+\beta_md_7)}\right]\\=&\frac{q_1p_2d_6}{\eta p_1q_2}\left[\mathcal{R}_p-1-\frac{\eta\beta_m\sigma_1p_1q_2}{q_1d_6(p_1d_1+\beta_md_7)}\right].\end{aligned}$$

Accordingly, $\dfrac{d\Delta_2}{dt}$ is given by

$$\begin{aligned}\frac{d\Delta_2}{dt} =&-d_1\int_\Gamma\frac{(U-U_2)^2}{U}\,\mathrm{d}x-\frac{eq_1p_2d_4}{\eta p_1q_2d_5}\int_\Gamma\frac{(Y-Y_2)^2}{Y}\,\mathrm{d}x+\beta_mU_2M_2\int_\Gamma\left(3-\frac{U_2}{U}-\frac{IM_2}{I_2M}-\frac{UI_2M}{U_2IM_2}\right)\mathrm{d}x\\&+\frac{q_1p_2d_6}{\eta p_1q_2}\left(\mathcal{R}_p-1-\frac{\eta\beta_m\sigma_1p_1q_2}{q_1d_6(p_1d_1+\beta_md_7)}\right)\int_\Gamma V\,\mathrm{d}x-D_UU_2\int_\Gamma\frac{\|\nabla U\|^2}{U^2}\,\mathrm{d}x\\&-D_II_2\int_\Gamma\frac{\|\nabla I\|^2}{I^2}\,\mathrm{d}x-\frac{1}{\eta}D_MM_2\int_\Gamma\frac{\|\nabla M\|^2}{M^2}\,\mathrm{d}x-\frac{eq_1p_2}{\eta p_1q_2d_5}D_YY_2\int_\Gamma\frac{\|\nabla Y\|^2}{Y^2}\,\mathrm{d}x\\&-\frac{q_1}{\eta p_1}D_ZZ_2\int_\Gamma\frac{\|\nabla Z\|^2}{Z^2}\,\mathrm{d}x.\end{aligned}$$

We observe that $\frac{d\Delta_2}{dt} \leq 0$ if $\mathcal{R}_p \leq 1 + \frac{\eta\beta_m\sigma_1 p_1 q_2}{q_1 d_6(p_1 d_1 + \beta_m d_7)}$. In addition, $\frac{d\Delta_2}{dt} = 0$ when $U = U_2$, $I = I_2$, $M = M_2$, $Y = Y_2$, and $V = 0$. We can prove that the elements of $K_2^{'}$ satisfy $N = 0$ and $Z = Z_2$. Consequently, $K_2^{'} = \{E_2\}$. Therefore, the global asymptotic stability of E_2 is followed by LIP when $\mathcal{R}_{1m} > 1$ and $\mathcal{R}_p \leq 1 + \frac{\eta\beta_m\sigma_1 p_1 q_2}{q_1 d_6(p_1 d_1 + \beta_m d_7)}$. □

Theorem 5. *Assume that $\mathcal{R}_{0v} > 1$. Then, the SARS-CoV-2 single-infection without immunity equilibrium E_3 is GAS when $\mathcal{R}_{0m} \leq 1$ and $\mathcal{R}_{1v} \leq 1$.*

Proof. Define

$$\begin{aligned}\widetilde{\Delta}_3(x,t) =& U_3\left(\frac{U}{U_3} - 1 - \ln\frac{U}{U_3}\right) + I + \frac{1}{\eta}M + \frac{eq_1p_2}{\eta p_1 q_2 d_5}Y_3\left(\frac{Y}{Y_3} - 1 - \ln\frac{Y}{Y_3}\right)\\ &+ \frac{eq_1p_2}{\eta p_1 q_2 d_5}N_3\left(\frac{N}{N_3} - 1 - \ln\frac{N}{N_3}\right) + \frac{q_1p_2}{\eta p_1 q_2}V_3\left(\frac{V}{V_3} - 1 - \ln\frac{V}{V_3}\right) + \frac{q_1}{\eta p_1}Z.\end{aligned}$$

Then, we obtain

$$\begin{aligned}\frac{\partial\widetilde{\Delta}_3}{\partial t} =& \left(1 - \frac{U_3}{U}\right)\left(D_U\Delta U + \sigma_1 - \beta_m UM - d_1U\right) + D_I\Delta I + \beta_m UM - d_2I\\ &+ \frac{1}{\eta}\left(D_M\Delta M + \eta d_2 I - q_1MZ - d_3M\right) + \frac{eq_1p_2}{\eta p_1q_2d_5}\left(1 - \frac{Y_3}{Y}\right)\left(D_Y\Delta Y + \sigma_2 - \beta_v YV - d_4Y\right)\\ &+ \frac{eq_1p_2}{\eta p_1q_2d_5}\left(1 - \frac{N_3}{N}\right)\left(D_N\Delta N + \beta_v YV - d_5N\right) + \frac{q_1p_2}{\eta p_1q_2}\left(1 - \frac{V_3}{V}\right)\left(D_V\Delta V + eN - q_2VZ - d_6V\right)\\ &+ \frac{q_1}{\eta p_1}\left(D_Z\Delta Z + p_1MZ + p_2VZ - d_7Z\right).\end{aligned} \tag{13}$$

By using the equilibrium conditions at E_3

$$\begin{cases}\sigma_1 = d_1U_3,\\ \sigma_2 = \beta_v Y_3V_3 + d_4Y_3,\\ \frac{eq_1p_2\beta_v}{\eta p_1q_2d_5}Y_3V_3 = \frac{eq_1p_2}{\eta p_1q_2}N_3,\\ \frac{eq_1p_2}{\eta p_1q_2}N_3 = \frac{q_1p_2d_6}{\eta p_1q_2}V_3,\end{cases}$$

the partial derivative in (13) is transformed to

$$\begin{aligned}\frac{\partial\widetilde{\Delta}_3}{\partial t} =& \left(1 - \frac{U_3}{U}\right)\left(d_1U_3 - d_1U\right) + \frac{eq_1p_2}{\eta p_1q_2d_5}\left(1 - \frac{Y_3}{Y}\right)\left(d_4Y_3 - d_4Y\right) + 3\frac{eq_1p_2\beta_v}{\eta p_1q_2d_5}\beta_v Y_3V_3\\ &- \frac{eq_1p_2}{\eta p_1q_2d_5}\beta_v Y_3V_3\frac{Y_3}{Y} - \frac{eq_1p_2}{\eta p_1q_2d_5}\beta_v Y_3V_3\frac{NV_3}{N_3V} - \frac{eq_1p_2}{\eta p_1q_2d_5}\beta_v Y_3V_3\frac{YN_3V}{Y_3NV_3} + \left(\beta_mU_3 - \frac{d_3}{\eta}\right)M\\ &+ \left(\frac{q_1p_2}{\eta p_1} - \frac{q_1d_7}{\eta p_1}\right)Z + \left(1 - \frac{U_3}{U}\right)D_U\Delta U + D_I\Delta I + \frac{1}{\eta}D_M\Delta M + \frac{eq_1p_2}{\eta p_1q_2d_5}\left(1 - \frac{Y_3}{Y}\right)D_Y\Delta Y\\ &+ \frac{eq_1p_2}{\eta p_1q_2d_5}\left(1 - \frac{N_3}{N}\right)D_N\Delta N + \frac{q_1p_2}{\eta p_1q_2}\left(1 - \frac{V_3}{V}\right)D_V\Delta V + \frac{q_1}{\eta p_1}D_Z\Delta Z.\end{aligned}$$

Accordingly, $\frac{d\Delta_3}{dt}$ is given by

$$\begin{aligned}\frac{d\Delta_3}{dt} =& -d_1\int_\Gamma \frac{(U-U_3)^2}{U}\,\mathrm{d}x - \frac{eq_1p_2d_4}{\eta p_1q_2d_5}\int_\Gamma \frac{(Y-Y_3)^2}{Y}\,\mathrm{d}x + \frac{eq_1p_2}{\eta p_1q_2d_5}\beta_v Y_3V_3\int_\Gamma\left(3-\frac{Y_3}{Y}-\frac{NV_3}{N_3V}-\frac{YN_3V}{Y_3NV_3}\right)\mathrm{d}x\\ &+\frac{d_3}{\eta}(\mathcal{R}_{0m}-1)\int_\Gamma M\,\mathrm{d}x + \frac{q_1(p_2d_4+\beta_v d_7)}{\eta p_1\beta_v}(\mathcal{R}_{1v}-1)\int_\Gamma Z\,\mathrm{d}x - D_UU_3\int_\Gamma\frac{\|\nabla U\|^2}{U^2}\,\mathrm{d}x\\ &-\frac{eq_1p_2}{\eta p_1q_2d_5}D_YY_3\int_\Gamma\frac{\|\nabla Y\|^2}{Y^2}\,\mathrm{d}x - \frac{eq_1p_2}{\eta p_1q_2d_5}D_NN_3\int_\Gamma\frac{\|\nabla N\|^2}{N^2}\,\mathrm{d}x - \frac{q_1p_2}{\eta p_1q_2}D_VV_3\int_\Gamma\frac{\|\nabla V\|^2}{V^2}\,\mathrm{d}x.\end{aligned}$$

This implies that $\frac{d\Delta_3}{dt}\le 0$ if $\mathcal{R}_{0m}\le 1$ and $\mathcal{R}_{1v}\le 1$. In addition, one can show that $\frac{d\Delta_3}{dt}=0$ when $U=U_3$, $I=0$, $M=0$, $Y=Y_3$, $N=N_3$, $V=V_3$, and $Z=0$. Thus, $K_3^{'}=\{E_3\}$. As a result, LIP insures the global asymptotic stability of E_3 when $\mathcal{R}_{0v}>1$, $\mathcal{R}_{0m}\le 1$ and $\mathcal{R}_{1v}\le 1$. □

Theorem 6. *Assume that $\mathcal{R}_{1v}>1$. Then, the SARS-CoV-2 single-infection with immunity equilibrium E_4 is GAS if $\mathcal{R}_{0m}+\frac{q_1d_6}{q_2d_3}\le 1+\frac{q_1d_6}{q_2d_3}\mathcal{R}_{1v}$.*

Proof. Consider

$$\begin{aligned}\widetilde{\Delta}_4(x,t) =& U_4\left(\frac{U}{U_4}-1-\ln\frac{U}{U_4}\right)+I+\frac{1}{\eta}M+\frac{eq_1p_2}{\eta p_1q_2d_5}Y_4\left(\frac{Y}{Y_4}-1-\ln\frac{Y}{Y_4}\right)+\frac{eq_1p_2}{\eta p_1q_2d_5}N_4\left(\frac{N}{N_4}-1-\ln\frac{N}{N_4}\right)\\ &+\frac{q_1p_2}{\eta p_1q_2}V_4\left(\frac{V}{V_4}-1-\ln\frac{V}{V_4}\right)+\frac{q_1}{\eta p_1}Z_4\left(\frac{Z}{Z_4}-1-\ln\frac{Z}{Z_4}\right).\end{aligned}$$

Then, we have

$$\begin{aligned}\frac{\partial\widetilde{\Delta}_4}{\partial t} =& \left(1-\frac{U_4}{U}\right)\left(D_U\Delta U+\sigma_1-\beta_mUM-d_1U\right)+D_I\Delta I+\beta_mUM-d_2I\\ &+\frac{1}{\eta}\left(D_M\Delta M+\eta d_2I-q_1MZ-d_3M\right)+\frac{eq_1p_2}{\eta p_1q_2d_5}\left(1-\frac{Y_4}{Y}\right)\left(D_Y\Delta Y+\sigma_2-\beta_vYV-d_4Y\right)\\ &+\frac{eq_1p_2}{\eta p_1q_2d_5}\left(1-\frac{N_4}{N}\right)\left(D_N\Delta N+\beta_vYV-d_5N\right)+\frac{q_1p_2}{\eta p_1q_2}\left(1-\frac{V_4}{V}\right)\left(D_V\Delta V+eN-q_2VZ-d_6V\right)\\ &+\frac{q_1}{\eta p_1}\left(1-\frac{Z_4}{Z}\right)\left(D_Z\Delta Z+p_1MZ+p_2VZ-d_7Z\right).\end{aligned}\tag{14}$$

The equilibrium conditions at E_4 can be written as

$$\begin{cases}\sigma_1=d_1U_4,\\ \sigma_2=\beta_vY_4V_4+d_4Y_4,\\ \frac{eq_1p_2\beta_v}{\eta p_1q_2d_5}Y_4V_4=\frac{eq_1p_2}{\eta p_1q_2}N_4,\\ \frac{eq_1p_2}{\eta p_1q_2}N_4=\frac{q_1p_2d_6}{\eta p_1q_2}V_4+\frac{q_1p_2}{\eta p_1}V_4Z_4,\\ \frac{q_1p_2}{\eta p_1}V_4Z_4=\frac{q_1d_7}{\eta p_1}Z_4.\end{cases}\tag{15}$$

By utilizing Equation (15) to collect terms of Equation (14), we obtain

$$\begin{aligned}\frac{\partial\widetilde{\Delta}_4}{\partial t} =& -\frac{d_1(U-U_4)^2}{U} - \frac{eq_1p_2d_4}{\eta p_1q_2d_5}\frac{(Y-Y_4)^2}{Y} + \frac{eq_1p_2}{\eta p_1q_2d_5}\beta_v Y_4V_4\left(3-\frac{Y_4}{Y}-\frac{NV_4}{N_4V}-\frac{YN_4V}{Y_4NV_4}\right)\\ &+(\beta_m U_4-\frac{d_3}{\eta}-\frac{q_1}{\eta}Z_4)M+\left(1-\frac{U_4}{U}\right)D_U\Delta U+D_I\Delta I+\frac{1}{\eta}D_M\Delta M+\frac{eq_1p_2}{\eta p_1q_2d_5}\left(1-\frac{Y_4}{Y}\right)D_Y\Delta Y\\ &+\frac{eq_1p_2}{\eta p_1q_2d_5}\left(1-\frac{N_4}{N}\right)D_N\Delta N+\frac{q_1p_2}{\eta p_1q_2}\left(1-\frac{V_4}{V}\right)D_V\Delta V+\frac{q_1}{\eta p_1}\left(1-\frac{Z_4}{Z}\right)D_Z\Delta Z.\end{aligned}$$

By using Equation (9), $\frac{d\Delta_4}{dt}$ is computed as

$$\begin{aligned}\frac{d\Delta_4}{dt} =& -d_1\int_\Gamma\frac{(U-U_4)^2}{U}\,\mathrm{d}x-\frac{eq_1p_2d_4}{\eta p_1q_2d_5}\int_\Gamma\frac{(Y-Y_4)^2}{Y}\,\mathrm{d}x+\frac{eq_1p_2}{\eta p_1q_2d_5}\beta_vY_4V_4\int_\Gamma\left(3-\frac{Y_4}{Y}-\frac{NV_4}{N_4V}-\frac{YN_4V}{Y_4NV_4}\right)\mathrm{d}x\\ &+\frac{d_3}{\eta}\left(\mathcal{R}_{0m}+\frac{q_1d_6}{q_2d_3}-1-\frac{q_1d_6}{q_2d_3}\mathcal{R}_{1v}\right)\int_\Gamma M\,\mathrm{d}x-D_UU_4\int_\Gamma\frac{\|\nabla U\|^2}{U^2}\,\mathrm{d}x-\frac{eq_1p_2}{\eta p_1q_2d_5}D_YY_4\int_\Gamma\frac{\|\nabla Y\|^2}{Y^2}\,\mathrm{d}x\\ &-\frac{eq_1p_2}{\eta p_1q_2d_5}D_NN_4\int_\Gamma\frac{\|\nabla N\|^2}{N^2}\,\mathrm{d}x-\frac{q_1p_2}{\eta p_1q_2}D_VV_4\int_\Gamma\frac{\|\nabla V\|^2}{V^2}\,\mathrm{d}x-\frac{q_1}{\eta p_1}D_ZZ_4\int_\Gamma\frac{\|\nabla Z\|^2}{Z^2}\,\mathrm{d}x.\end{aligned}$$

Therefore, $\frac{d\Delta_4}{dt}\leq 0$ if $\mathcal{R}_{0m}+\frac{q_1d_6}{q_2d_3}\leq 1+\frac{q_1d_6}{q_2d_3}\mathcal{R}_{1v}$. Furthermore, $\frac{d\Delta_4}{dt}=0$ when $U=U_4$, $M=0$, $Y=Y_4$, $N=N_4$, and $V=V_4$. One can show that $K_4'=\{E_4\}$. By LIP, the equilibrium E_4 is GAS if $\mathcal{R}_{1v}>1$ and $\mathcal{R}_{0m}+\frac{q_1d_6}{q_2d_3}\leq 1+\frac{q_1d_6}{q_2d_3}\mathcal{R}_{1v}$. □

Theorem 7. *Assume that $\mathcal{R}_{0m}>1$ and $\mathcal{R}_{0v}>1$. Then, the malaria/SARS-CoV-2 coinfection without immunity equilibrium E_5 is GAS if $\mathcal{R}_{0m}+\frac{e\beta_m\sigma_2p_2}{p_1d_1d_5d_6}\leq 1+\frac{\beta_m(p_2d_4+\beta_vd_7)}{\beta_vp_1d_1}$.*

Proof. Define

$$\begin{aligned}\widetilde{\Delta}_5(x,t) =& U_5\left(\frac{U}{U_5}-1-\ln\frac{U}{U_5}\right)+I_5\left(\frac{I}{I_5}-1-\ln\frac{I}{I_5}\right)+\frac{1}{\eta}M_5\left(\frac{M}{M_5}-1-\ln\frac{M}{M_5}\right)+\frac{eq_1p_2}{\eta p_1q_2d_5}Y_5\left(\frac{Y}{Y_5}-1-\ln\frac{Y}{Y_5}\right)\\ &+\frac{eq_1p_2}{\eta p_1q_2d_5}N_5\left(\frac{N}{N_5}-1-\ln\frac{N}{N_5}\right)+\frac{q_1p_2}{\eta p_1q_2}V_5\left(\frac{V}{V_5}-1-\ln\frac{V}{V_5}\right)+\frac{q_1}{\eta p_1}Z.\end{aligned}$$

Then, we obtain

$$\begin{aligned}\frac{\partial\widetilde{\Delta}_5}{\partial t} =& \left(1-\frac{U_5}{U}\right)\left(D_U\Delta U+\sigma_1-\beta_mUM-d_1U\right)+\left(1-\frac{I_5}{I}\right)\left(D_I\Delta I+\beta_mUM-d_2I\right)\\ &+\frac{1}{\eta}\left(1-\frac{M_5}{M}\right)\left(D_M\Delta M+\eta d_2I-q_1MZ-d_3M\right)+\frac{eq_1p_2}{\eta p_1q_2d_5}\left(1-\frac{Y_5}{Y}\right)\left(D_Y\Delta Y+\sigma_2-\beta_vYV-d_4Y\right)\\ &+\frac{eq_1p_2}{\eta p_1q_2d_5}\left(1-\frac{N_5}{N}\right)\left(D_N\Delta N+\beta_vYV-d_5N\right)+\frac{q_1p_2}{\eta p_1q_2}\left(1-\frac{V_5}{V}\right)\left(D_V\Delta V+eN-q_2VZ-d_6V\right)\\ &+\frac{q_1}{\eta p_1}\left(D_Z\Delta Z+p_1MZ+p_2VZ-d_7Z\right).\end{aligned}\tag{16}$$

The equilibrium conditions at E_5 can be written as

$$\begin{cases} \sigma_1 = d_1 U_5 + \beta_m U_5 M_5, \\ \beta_m U_5 M_5 = d_2 I_5, \\ d_2 I_5 = \dfrac{d_3}{\eta} M_5, \\ \sigma_2 = \beta_v Y_5 V_5 + d_4 Y_5, \\ \dfrac{e q_1 p_2 \beta_v}{\eta p_1 q_2 d_5} Y_5 V_5 = \dfrac{e q_1 p_2}{\eta p_1 q_2} N_5, \\ \dfrac{e q_1 p_2}{\eta p_1 q_2} N_5 = \dfrac{q_1 p_2 d_6}{\eta p_1 q_2} V_5. \end{cases}$$

By using the above conditions, the derivative in (16) becomes

$$\begin{aligned} \frac{\partial \widetilde{\Delta}_5}{\partial t} =& - \frac{d_1 (U - U_5)^2}{U} - \frac{e q_1 p_2 d_4}{\eta p_1 q_2 d_5} \frac{(Y - Y_5)^2}{Y} + \beta_m U_5 M_5 \left(3 - \frac{U_5}{U} - \frac{I M_5}{I_5 M} - \frac{U I_5 U}{U_5 I M_5} \right) \\ &+ \frac{e q_1 p_2}{\eta p_1 q_2 d_5} \beta_v Y_5 V_5 \left(3 - \frac{Y_5}{Y} - \frac{N V_5}{N_5 V} - \frac{Y N_5 V}{Y_5 N V_5} \right) + \left(\frac{q_1}{\eta} M_5 + \frac{q_1 p_2}{\eta p_1} V_5 - \frac{q_1 d_7}{\eta p_1} \right) Z \\ &+ \left(1 - \frac{U_5}{U} \right) D_U \Delta U + \left(1 - \frac{I_5}{I} \right) D_I \Delta I + \frac{1}{\eta} \left(1 - \frac{M_5}{M} \right) D_M \Delta M + \frac{e q_1 p_2}{\eta p_1 q_2 d_5} \left(1 - \frac{Y_5}{Y} \right) D_Y \Delta Y \\ &+ \frac{e q_1 p_2}{\eta p_1 q_2 d_5} \left(1 - \frac{N_5}{N} \right) D_N \Delta N + \frac{q_1 p_2}{\eta p_1 q_2} \left(1 - \frac{V_5}{V} \right) D_V \Delta V + \frac{q_1}{\eta p_1} D_Z \Delta Z. \end{aligned} \tag{17}$$

To evaluate the fifth term in (17), we calculate

$$\begin{aligned} \frac{q_1}{\eta} M_5 + \frac{q_1 p_2}{\eta p_1} V_5 - \frac{q_1 d_7}{\eta p_1} =& \frac{q_1 \sigma_1}{d_3} + \frac{e q_1 \sigma_2 p_2}{\eta p_1 d_5 d_6} - \frac{q_1 d_1}{\eta \beta_m} - \frac{q_1 p_2 d_4}{\eta p_1 \beta_v} - \frac{q_1 d_7}{\eta p_1} \\ =& \frac{q_1 d_1}{\eta \beta_m} \left[\frac{\eta \sigma_1 \beta_m}{d_1 d_3} + \frac{e \beta_m \sigma_2 p_2}{p_1 d_1 d_5 d_6} - 1 - \frac{\beta_m (p_2 d_4 + \beta_v d_7)}{\beta_v p_1 d_1} \right] \\ =& \frac{q_1 d_1}{\eta \beta_m} \left[\mathcal{R}_{0m} + \frac{e \beta_m \sigma_2 p_2}{p_1 d_1 d_5 d_6} - 1 - \frac{\beta_m (p_2 d_4 + \beta_v d_7)}{\beta_v p_1 d_1} \right]. \end{aligned}$$

Accordingly, $\dfrac{d\Delta_5}{dt}$ is provided as

$$\begin{aligned} \frac{d\Delta_5}{dt} =& - d_1 \int_\Gamma \frac{(U - U_5)^2}{U} \, \mathrm{d}x - \frac{e q_1 p_2 d_4}{\eta p_1 q_2 d_5} \int_\Gamma \frac{(Y - Y_5)^2}{Y} \, \mathrm{d}x + \beta_m U_5 M_5 \int_\Gamma \left(3 - \frac{U_5}{U} - \frac{I M_5}{I_5 M} - \frac{U I_5 M}{U_5 I M_5} \right) \mathrm{d}x \\ &+ \frac{e q_1 p_2}{\eta p_1 q_2 d_5} \beta_v Y_5 V_5 \int_\Gamma \left(3 - \frac{Y_5}{Y} - \frac{N V_5}{N_5 V} - \frac{Y N_5 V}{Y_5 N V_5} \right) \mathrm{d}x + \left(\mathcal{R}_{0m} + \frac{e \beta_m \sigma_2 p_2}{p_1 d_1 d_5 d_6} - 1 - \frac{\beta_m (p_2 d_4 + \beta_v d_7)}{\beta_v p_1 d_1} \right) \int_\Gamma Z \, \mathrm{d}x \\ &- D_U U_5 \int_\Gamma \frac{\| \nabla U \|^2}{U^2} \, \mathrm{d}x - D_I I_5 \int_\Gamma \frac{\| \nabla I \|^2}{I^2} \, \mathrm{d}x - \frac{1}{\eta} D_M M_5 \int_\Gamma \frac{\| \nabla M \|^2}{M^2} \, \mathrm{d}x - \frac{e q_1 p_2}{\eta p_1 q_2 d_5} D_Y Y_5 \int_\Gamma \frac{\| \nabla Y \|^2}{Y^2} \, \mathrm{d}x \\ &- \frac{e q_1 p_2}{\eta p_1 q_2 d_5} D_N N_5 \int_\Gamma \frac{\| \nabla N \|^2}{N^2} \, \mathrm{d}x - \frac{q_1 p_2}{\eta p_1 q_2} D_V V_5 \int_\Gamma \frac{\| \nabla V \|^2}{V^2} \, \mathrm{d}x. \end{aligned}$$

Hence, we have $\dfrac{d\Delta_5}{dt} \leq 0$ if $\mathcal{R}_{0m} + \dfrac{e \beta_m \sigma_2 p_2}{p_1 d_1 d_5 d_6} \leq 1 + \dfrac{\beta_m (p_2 d_4 + \beta_v d_7)}{\beta_v p_1 d_1}$. In addition, $\dfrac{d\Delta_5}{dt} = 0$ when $U = U_5$, $I = I_5$, $M = M_5$, $Y = Y_5$, $N = N_5$, $V = V_5$, and $Z = 0$. Thus, $K_5' = \{E_5\}$ and, according to LIP, E_5 is GAS if $\mathcal{R}_{0m} > 1$, $\mathcal{R}_{0v} > 1$, and $\mathcal{R}_{0m} + \dfrac{e \beta_m \sigma_2 p_2}{p_1 d_1 d_5 d_6} \leq 1 + \dfrac{\beta_m (p_2 d_4 + \beta_v d_7)}{\beta_v p_1 d_1}$. □

Theorem 8. *Suppose that* $\mathcal{R}_p > 1 + \frac{\eta\beta_m\sigma_1 p_1 q_2}{q_1 d_6(p_1 d_1 + \beta_m d_7)}$, $\mathcal{R}_{0m} + \frac{q_1 d_6}{q_2 d_3} > 1 + \frac{q_1 d_6}{q_2 d_3}\mathcal{R}_{1v}$, *and* $\mathcal{R}_{0m} + \frac{e\beta_m\sigma_2 p_2}{p_1 d_1 d_5 d_6} > 1 + \frac{\beta_m(p_2 d_4 + \beta_v d_7)}{\beta_v p_1 d_1}$. *Then, the malaria/SARS-CoV-2 coinfection with immunity equilibrium* E_6 *is GAS.*

Proof. Consider

$$\begin{aligned}\widetilde{\Delta}_6(x,t) =& U_6\left(\frac{U}{U_6} - 1 - \ln\frac{U}{U_6}\right) + I_6\left(\frac{I}{I_6} - 1 - \ln\frac{I}{I_6}\right) + \frac{1}{\eta}M_6\left(\frac{M}{M_6} - 1 - \ln\frac{M}{M_6}\right)\\ &+ \frac{eq_1p_2}{\eta p_1 q_2 d_5}Y_6\left(\frac{Y}{Y_6} - 1 - \ln\frac{Y}{Y_6}\right) + \frac{eq_1p_2}{\eta p_1 q_2 d_5}N_6\left(\frac{N}{N_6} - 1 - \ln\frac{N}{N_6}\right)\\ &+ \frac{q_1p_2}{\eta p_1 q_2}V_6\left(\frac{V}{V_6} - 1 - \ln\frac{V}{V_6}\right) + \frac{q_1}{\eta p_1}Z_6\left(\frac{Z}{Z_6} - 1 - \ln\frac{Z}{Z_6}\right).\end{aligned}$$

Then, we obtain

$$\begin{aligned}\frac{\partial\widetilde{\Delta}_6}{\partial t} =& \left(1 - \frac{U_6}{U}\right)\left(D_U\Delta U + \sigma_1 - \beta_m UM - d_1U\right) + \left(1 - \frac{I_6}{I}\right)\left(D_I\Delta I + \beta_m UM - d_2I\right)\\ &+ \frac{1}{\eta}\left(1 - \frac{M_6}{M}\right)\left(D_M\Delta M + \eta d_2 I - q_1MZ - d_3M\right) + \frac{eq_1p_2}{\eta p_1 q_2 d_5}\left(1 - \frac{Y_6}{Y}\right)\left(D_Y\Delta Y + \sigma_2 - \beta_v YV - d_4Y\right)\\ &+ \frac{eq_1p_2}{\eta p_1 q_2 d_5}\left(1 - \frac{N_6}{N}\right)\left(D_N\Delta N + \beta_v YV - d_5N\right) + \frac{q_1p_2}{\eta p_1 q_2}\left(1 - \frac{V_6}{V}\right)\left(D_V\Delta V + eN - q_2VZ - d_6V\right)\\ &+ \frac{q_1}{\eta p_1}\left(1 - \frac{Z_6}{Z}\right)\left(D_Z\Delta Z + p_1MZ + p_2VZ - d_7Z\right).\end{aligned}$$

By using the equilibrium conditions at E_6,

$$\begin{cases}\sigma_1 = d_1U_6 + \beta_m U_6M_6,\\ \beta_m U_6M_6 = d_2I_6,\\ d_2I_6 = \frac{d_3}{\eta}M_6 + \frac{q_1}{\eta}M_6Z_6,\\ \sigma_2 = \beta_v Y_6V_6 + d_4Y_6,\\ \frac{eq_1p_2\beta_v}{\eta p_1 q_2 d_5}Y_6V_6 = \frac{eq_1p_2}{\eta p_1 q_2}N_6,\\ \frac{eq_1p_2}{\eta p_1 q_2}N_6 = \frac{q_1p_2d_6}{\eta p_1 q_2}V_6 + \frac{q_1p_2}{\eta p_1}V_6Z_6,\\ \frac{q_1}{\eta}M_6Z_6 + \frac{q_1p_2}{\eta p_1}V_6Z_6 = \frac{q_1d_7}{\eta p_1}Z_6,\end{cases}$$

and the $\frac{d\Delta_6}{dt}$ is given by

$$\begin{aligned}\frac{d\Delta_6}{dt} =& -d_1\int_\Gamma\frac{(U-U_6)^2}{U}\,\mathrm{d}x - \frac{eq_1p_2d_4}{\eta p_1q_2d_5}\int_\Gamma\frac{(Y-Y_6)^2}{Y}\,\mathrm{d}x + \beta_mU_6M_6\int_\Gamma\left(3 - \frac{U_6}{U} - \frac{IM_6}{I_6M} - \frac{UI_6M}{U_6IM_6}\right)\mathrm{d}x\\ &+ \frac{eq_1p_2}{\eta p_1q_2d_5}\beta_vY_6V_6\int_\Gamma\left(3 - \frac{Y_6}{Y} - \frac{NV_6}{N_6V} - \frac{YN_6V}{Y_6NV_6}\right)\mathrm{d}x - D_UU_6\int_\Gamma\frac{\|\nabla U\|^2}{U^2}\,\mathrm{d}x - D_II_6\int_\Gamma\frac{\|\nabla I\|^2}{I^2}\,\mathrm{d}x\\ &- \frac{1}{\eta}D_MM_6\int_\Gamma\frac{\|\nabla M\|^2}{M^2}\,\mathrm{d}x - \frac{eq_1p_2}{\eta p_1q_2d_5}D_YY_6\int_\Gamma\frac{\|\nabla Y\|^2}{Y^2}\,\mathrm{d}x - \frac{eq_1p_2}{\eta p_1q_2d_5}D_NN_6\int_\Gamma\frac{\|\nabla N\|^2}{N^2}\,\mathrm{d}x\\ &- \frac{q_1p_2}{\eta p_1q_2}D_VV_6\int_\Gamma\frac{\|\nabla V\|^2}{V^2}\,\mathrm{d}x - \frac{q_1}{\eta p_1}D_ZZ_6\int_\Gamma\frac{\|\nabla Z\|^2}{Z^2}\,\mathrm{d}x.\end{aligned}$$

Therefore, we have $\frac{d\Delta_6}{dt} \leq 0$. Furthermore, we have $\frac{d\Delta_6}{dt} = 0$ when $U = U_6$, $I = I_6$, $M = M_6$, $Y = Y_6$, $N = N_6$, $V = V_6$, and $Z = Z_6$. Thus, $K_6^{'} = \{E_6\}$. It follows from LIP that E_6 is GAS when $\mathcal{R}_p > 1 + \frac{\eta\beta_m\sigma_1 p_1 q_2}{q_1 d_6(p_1 d_1 + \beta_m d_7)}$, $\mathcal{R}_{0m} + \frac{q_1 d_6}{q_2 d_3} > 1 + \frac{q_1 d_6}{q_2 d_3}\mathcal{R}_{1v}$, and $\mathcal{R}_{0m} + \frac{e\beta_m\sigma_2 p_2}{p_1 d_1 d_5 d_6} > 1 + \frac{\beta_m(p_2 d_4 + \beta_v d_7)}{\beta_v p_1 d_1}$. □

5. Numerical Simulations

In this section, we execute some numerical simulations to visualize the analytical results gained previously. The MATLAB PDE solver (pdepe) is used to solve the equations (see the Supplementary File S1 pdex30.m). The spatial domain is selected as $\Gamma = [0, 2]$ with step size $\Delta x = 0.02$ and time step size $\Delta t = 0.1$. The initial conditions of model (1) are taken as:

$$U(x,0) = 5(1 + 0.2\cos^2(\pi x)), \quad I(x,0) = 0.0001(1 + 0.2\cos^2(\pi x)), \quad M(x,0) = 0.0002(1 + 0.2\cos^2(\pi x)),$$
$$Y(x,0) = 10(1 + 0.2\cos^2(\pi x)), \quad N(x,0) = 0.02(1 + 0.2\cos^2(\pi x)) \quad V(x,0) = 0.01(1 + 0.2\cos^2(\pi x)),$$
$$Z(x,0) = 0.1 \times 10^{10}(1 + 0.2\cos^2(\pi x)), \quad x \in [0, 2].$$

The values are assumed based on previous studies [8,48]. The results are classified into seven cases corresponding to the global stability of each equilibrium point. These cases are obtained by varying five parameters β_m, β_v, p_1, p_2, and d_7, while the rest of the parameters take fixed values as shown in Table 1. We used the values of some parameters which are given in the literature to perform our numerical simulations. We mention that these values are taken from studies for SARS-CoV-2 single-infection and malaria single-infection. To the best of our knowledge, till now, there has been no available data (e.g., the concentrations of SARS-CoV-2 particles, merozoites, antibodies, etc.) from SARS-CoV-2 and malaria coinfection patients. Therefore, estimating the parameters of the coinfection model is sill open for future work.

Table 1. Model parameters.

Parameter	Definition	Value	Reference
σ_1	Production rate of healthy RBCs	2.5×10^8	[21]
σ_2	Recruitment rate of healthy ECs	0.02241	[33]
β_m	Incidence rate constant of RBCs	Varied	–
β_v	Incidence rate constant of ECs	Varied	–
η	Number of merozoites produced from an infected RBC	16	[20]
q_1	Removal rate constant of merozoites by antibodies	10^{-8}	[21]
q_2	Removal rate constant of SARS-CoV-2 particles by antibodies	4.88×10^{-8}	[49]
e	Generation rate constant of SARS-CoV-2 by infected ECs	0.24	[33]
p_1	Proliferation rate constant of antibodies by merozoites	Varied	–
p_2	Proliferation rate constant of antibodies by SARS-CoV-2	Varied	–
d_1	Death rate constant of healthy RBCs	0.025	[21]
d_2	Death rate constant of infected RBCs	0.5	[26]
d_3	Death rate constant of merozoites	48	[21]
d_4	Death rate constant of healthy ECs	10^{-3}	[33]
d_5	Death rate constant of infected ECs	0.11	[33]
d_6	Death rate constant of SARS-CoV-2 particles	5.36	[33]
d_7	Death rate constant of antibodies	Varied	–
D_U	Diffusion coefficient of healthy RBCs	0.1	Assumed
D_I	Diffusion coefficient of infected RBCs	0.1	Assumed
D_M	Diffusion coefficient of merozoites	0.2	Assumed
D_Y	Diffusion coefficient of healthy ECs	0.01	Assumed
D_N	Diffusion coefficient of infected ECs	0.01	Assumed
D_V	Diffusion coefficient of SARS-CoV-2 particles	0.2	Assumed
D_Z	Diffusion coefficient of antibodies	0.2	Assumed

Now, we have the following cases:

(1) The varied parameters are $(\beta_m, \beta_v, p_1, p_2, d_7) = (2 \times 10^{-10}, 0.1, 3 \times 10^{-8}, 0.96, 0.2)$. This yields $\mathcal{R}_{0m} = 0.6667 < 1$ and $\mathcal{R}_{0v} = 0.9122 < 1$. This implies that the equilibrium $E_0 = (10 \times 10^9, 0, 0, 22.41, 0, 0, 0)$ is GAS (see Figure 1), which agrees with Theorem 2. This simulates an individual who has recovered from both malaria and SARS-CoV-2 infections.

(2) The selected parameters are $(\beta_m, \beta_v, p_1, p_2, d_7) = (2 \times 10^{-9}, 0.1, 2 \times 10^{-9}, 0.96, 0.2)$. Then, we obtain $\mathcal{R}_{0m} = 6.6667 > 1$, $\mathcal{R}_{0v} = 0.9122 < 1$, and $\mathcal{R}_{1m} = 0.7407 < 1$. Figure 2 shows that the numerical results agree with the analytical results of Theorem 4. The equilibrium $E_1 = (1.5 \times 10^9, 4.25 \times 10^8, 7.08 \times 10^7, 22.41, 0, 0, 0)$ is GAS. This case describes a patient who only has malaria with inactive antibody immune response.

(3) The varied parameters are $(\beta_m, \beta_v, p_1, p_2, d_7) = (2 \times 10^{-9}, 0.1, 3 \times 10^{-8}, 0.96, 0.2)$. This yields $\mathcal{R}_{1m} = 4.3478 > 1$ and $\mathcal{R}_p = 44.6137 < 1 + \dfrac{\eta \beta_m \sigma_1 p_1 q_2}{q_1 d_6 (p_1 d_1 + \beta_m d_7)} = 191.0065$. From Figure 3, we see that the equilibrium $E_2 = (6.522 \times 10^9, 1.739 \times 10^8, 6.667 \times 10^6, 22.41, 0, 0, 1.607 \times 10^{10})$ is GAS, which illustrates Theorem 4. This case represents a patient who has only malaria with an active antibody immune response.

(4) By choosing $(\beta_m, \beta_v, p_1, p_2, d_7) = (2 \times 10^{-10}, 0.9, 3 \times 10^{-8}, 0.96, 0.2)$, we obtain $\mathcal{R}_{0v} = 8.2099 > 1$, $\mathcal{R}_{0m} = 0.6667 < 1$, and $\mathcal{R}_{1v} = 0.0436 < 1$. Figure 4 illustrates the global asymptotic stability of the equilibrium $E_3 = (10 \times 10^9, 0, 0, 2.73, 0.1789, 0.008, 0)$ as given by Theorem 5. The patient in this situation suffers from SARS-CoV-2 single-infection with inactive immunity.

(5) By selecting $(\beta_m, \beta_v, p_1, p_2, d_7) = (2 \times 10^{-10}, 0.9, 3 \times 10^{-8}, 3.9, 0.01)$ we obtain $\mathcal{R}_{1v} = 2.4821 > 1$, $\mathcal{R}_{0m} + \dfrac{q_1 d_6}{q_2 d_3} = 0.6895 < 1 + \dfrac{e \beta_v q_1 \sigma_2 p_2}{q_2 d_3 d_5 (p_2 d_4 + \beta_v d_7)} = 1.0568$. Accordingly, the equilibrium $E_4 = (10 \times 10^9, 0, 0, 6.775, 0.1421, 0.0026, 1.628 \times 10^8)$ is GAS (see Figure 5). This result comes in agreement with Theorem 6. The patient in this situation has SARS-CoV-2 single-infection with active immunity. The activation of the antibody immunity causes a reduction in the number of SARS-CoV-2 particles.

(6) We take $(\beta_m, \beta_v, p_1, p_2, d_7) = (4 \times 10^{-10}, 0.9, 3 \times 10^{-8}, 0.96, 0.8)$. This gives $\mathcal{R}_{0m} = 1.3333 > 1$, $\mathcal{R}_{0v} = 8.2099 > 1$, and $\mathcal{R}_{0m} + \dfrac{e \beta_m \sigma_2 p_2}{p_1 d_1 d_5 d_6} = 1.338 < 1 + \dfrac{\beta_m (p_2 d_4 + \beta_v d_7)}{\beta_v p_1 d_1} = 1.4272$. Thus, the equilibrium $E_5 = (7.5 \times 10^9, 1.25 \times 10^8, 2.08 \times 10^7, 2.73, 0.1789, 0.008, 0)$ is GAS (see Figure 6), which agrees with Theorem 7. Here, the coinfection of malaria and COVID-19 occurs but with inactive antibody immunity. The inactivation of immunity enhances the replication of both SARS-CoV-2 particles and malaria merozoites, which worsens the health state of the patient.

(7) We select $(\beta_m, \beta_v, p_1, p_2, d_7) = (4 \times 10^{-10}, 3.9, 3 \times 10^{-8}, 0.5, 0.4)$. In this case, the threshold parameters are given as $\mathcal{R}_p = 79.2777 > 1 + \dfrac{\eta \beta_m \sigma_1 p_1 q_2}{q_1 d_6 (p_1 d_1 + \beta_m d_7)} = 49.0236$, $\mathcal{R}_{0m} + \dfrac{q_1 d_6}{q_2 d_3} = 1.3562 > 1 + \dfrac{e \beta_v q_1 \sigma_2 p_2}{q_2 d_3 d_5 (p_2 d_4 + \beta_v d_7)} = 1.0003$, and $\mathcal{R}_{0m} + \dfrac{e \beta_m \sigma_2 p_2}{p_1 d_1 d_5 d_6} = 1.3358 > 1 + \dfrac{\beta_m (p_2 d_4 + \beta_v d_7)}{\beta_v p_1 d_1} = 1.2134$. In line with Theorem 8, the equilibrium $E_6 = (8.244 \times 10^9, 8.78 \times 10^7, 1.33 \times 10^7, 3.36, 0.17, 0.0015, 4.76 \times 10^8)$ is GAS (see Figure 7). Under these circumstances, the coinfection of malaria and COVID-19 occurs with active antibody immunity. This action works on reducing the concentrations of both malaria merozoites and SARS-CoV-2 particles.

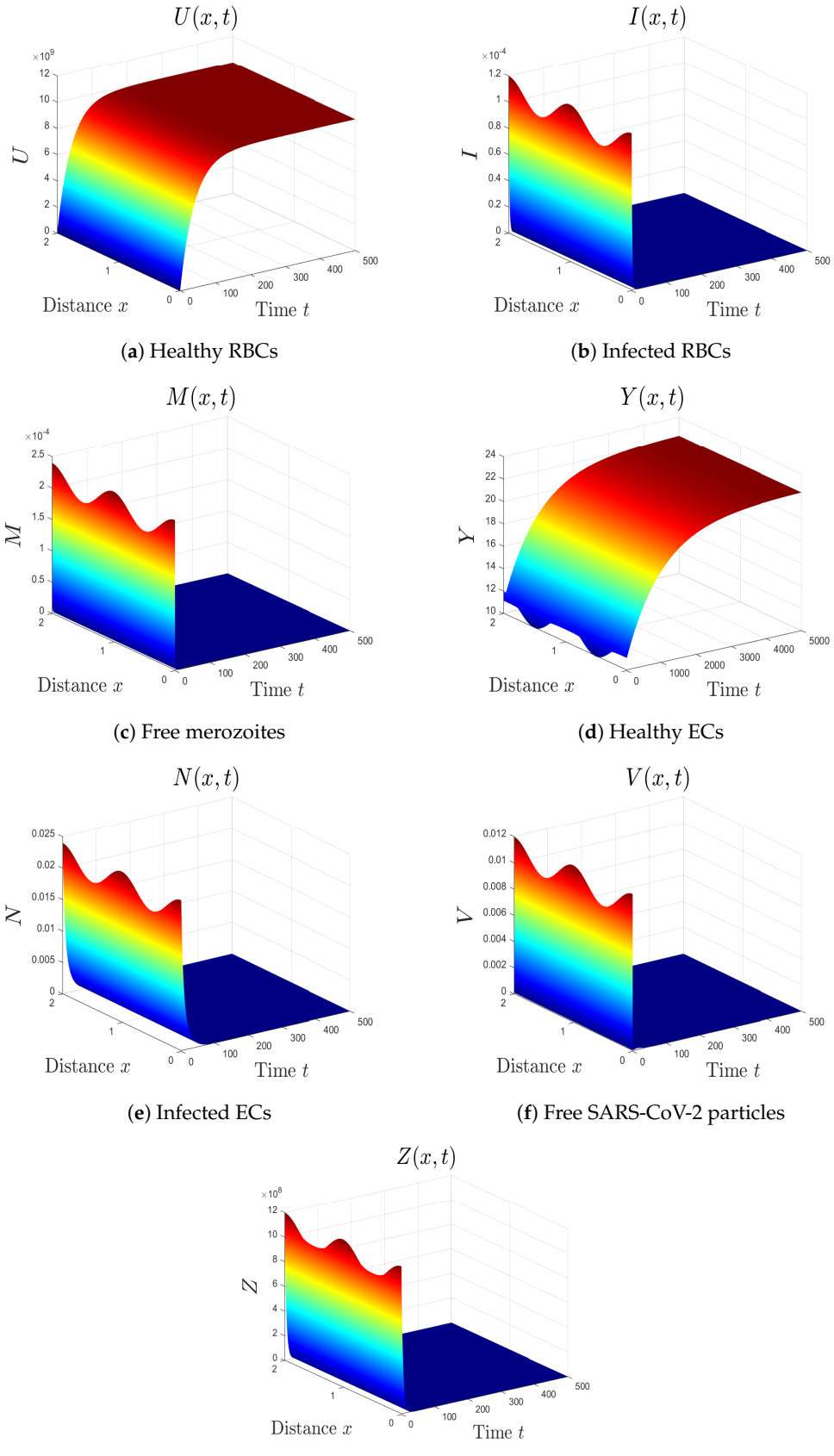

(**a**) Healthy RBCs

(**b**) Infected RBCs

(**c**) Free merozoites

(**d**) Healthy ECs

(**e**) Infected ECs

(**f**) Free SARS-CoV-2 particles

(**g**) Antibodies

Figure 1. Simulation of system (1) for $(\beta_m, \beta_v, p_1, p_2, d_7) = (2 \times 10^{-10}, 0.1, 3 \times 10^{-8}, 0.96, 0.2)$. The uninfected equilibrium $E_0 = (10 \times 10^9, 0, 0, 22.41, 0, 0, 0)$ is GAS.

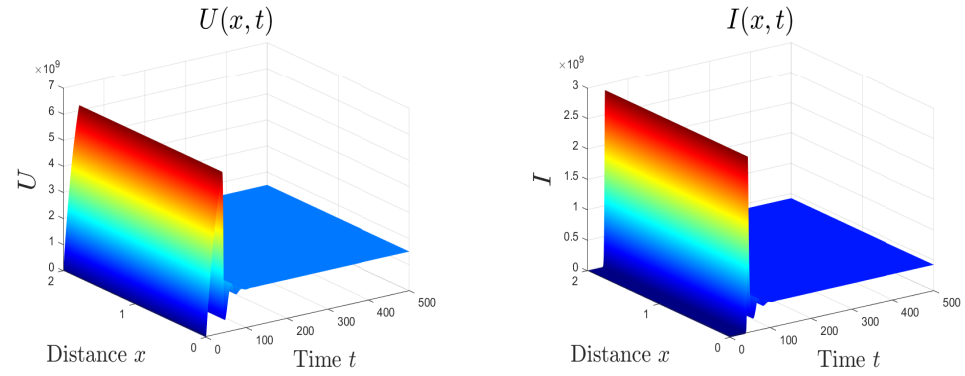

(**a**) Healthy RBCs

(**b**) Infected RBCs

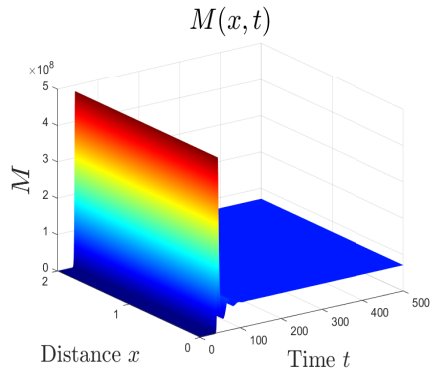

(**c**) Free merozoites

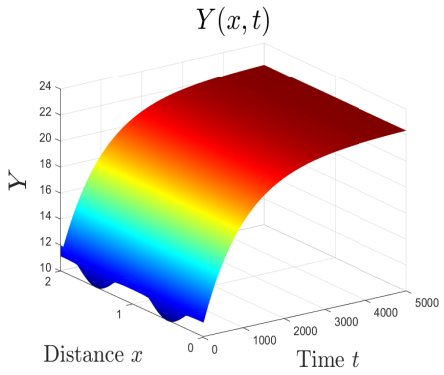

(**d**) Healthy ECs

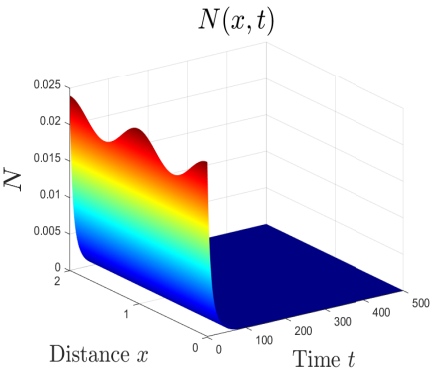

(**e**) Infected ECs

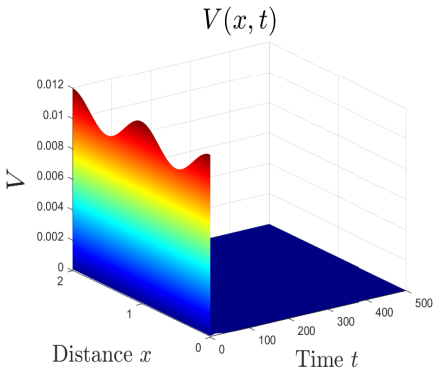

(**f**) Free SARS-CoV-2 particles

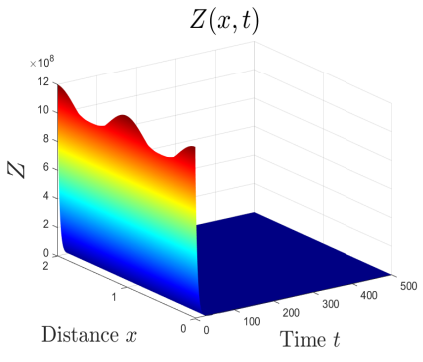

(**g**) Antibodies

Figure 2. Simulation of system (1) for $(\beta_m, \beta_v, p_1, p_2, d_7) = (2 \times 10^{-9}, 0.1, 2 \times 10^{-9}, 0.96, 0.2)$. The equilibrium $E_1 = (1.5 \times 10^9, 4.25 \times 10^8, 7.08 \times 10^7, 22.41, 0, 0, 0)$ is GAS.

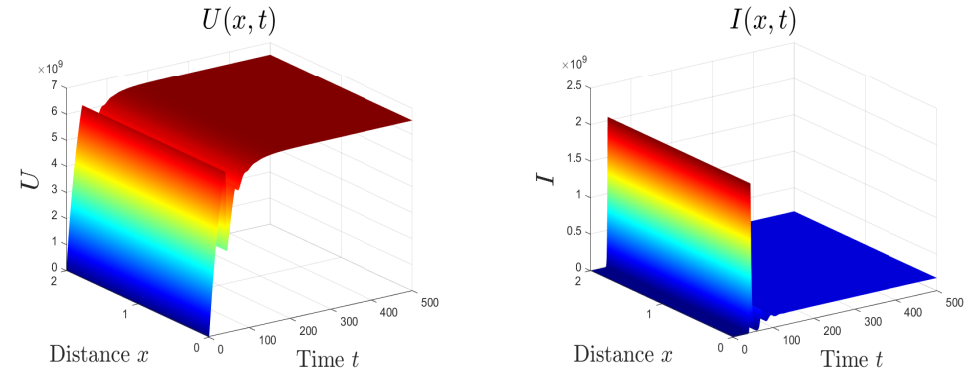

(**a**) Healthy RBCs

(**b**) Infected RBCs

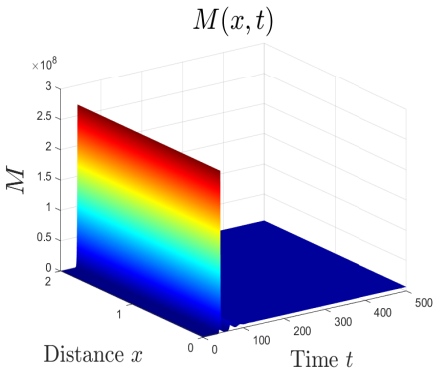

(**c**) Free merozoites

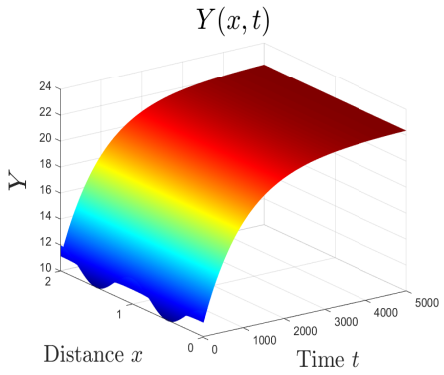

(**d**) Healthy ECs

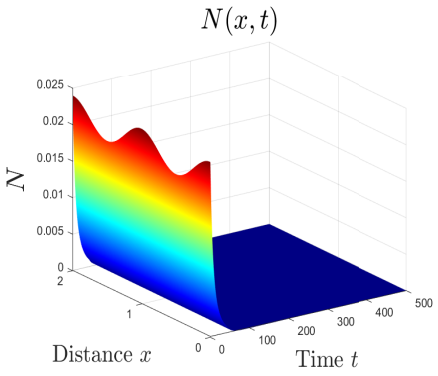

(**e**) Infected ECs

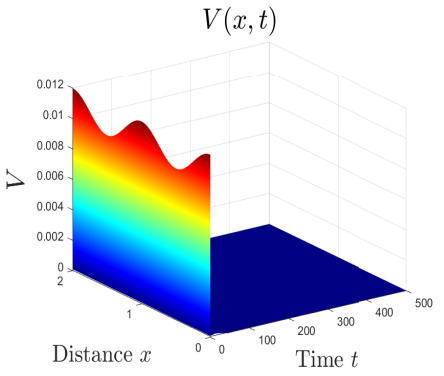

(**f**) Free SARS-CoV-2 particles

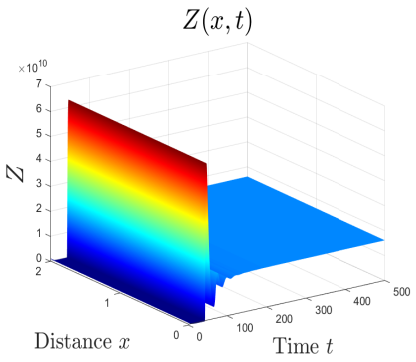

(**g**) Antibodies

Figure 3. Simulation of system (1) for $(\beta_m, \beta_v, p_1, p_2, d_7) = (2 \times 10^{-9}, 0.1, 3 \times 10^{-8}, 0.96, 0.2)$. The equilibrium $E_2 = (6.522 \times 10^9, 1.739 \times 10^8, 6.667 \times 10^6, 22.41, 0, 0, 1.607 \times 10^{10})$ is GAS.

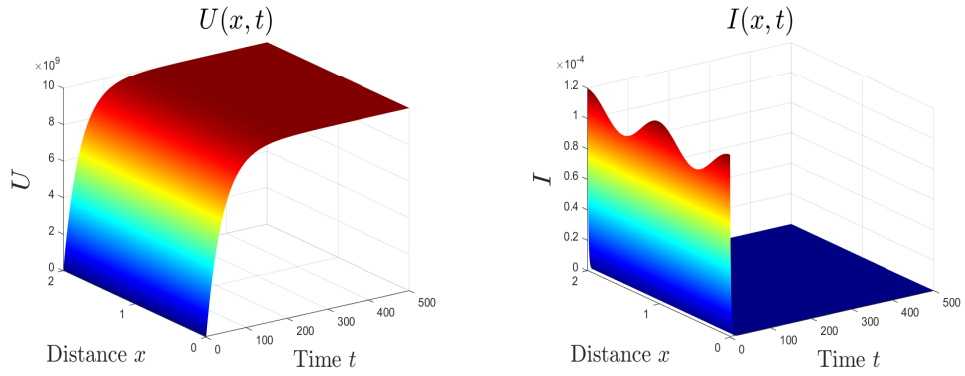

(**a**) Healthy RBCs

(**b**) Infected RBCs

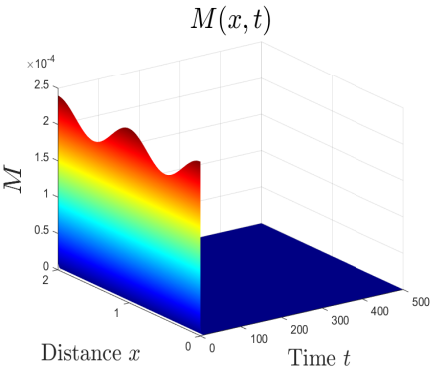

(**c**) Free merozoites

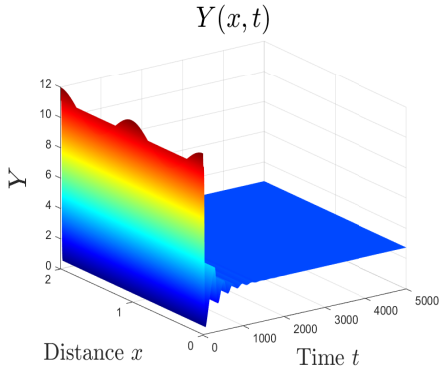

(**d**) Healthy ECs

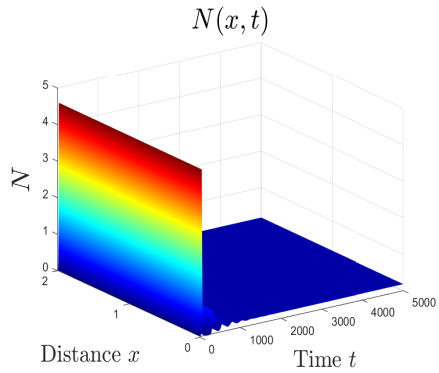

(**e**) Infected ECs

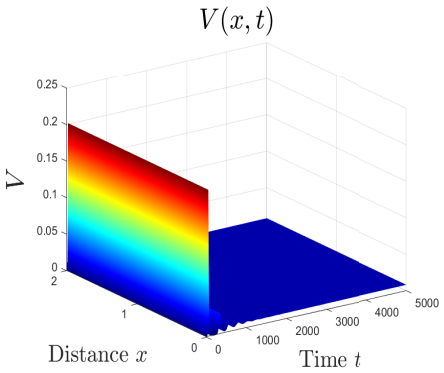

(**f**) Free SARS-CoV-2 particles

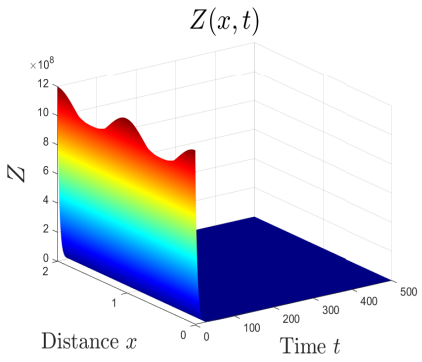

(**g**) Antibodies

Figure 4. Simulation of system (1) for $(\beta_m, \beta_v, p_1, p_2, d_7) = (2 \times 10^{-10}, 0.9, 3 \times 10^{-8}, 0.96, 0.2)$. The equilibrium $E_3 = (10 \times 10^9, 0, 0, 2.73, 0.1789, 0.008, 0)$ is GAS.

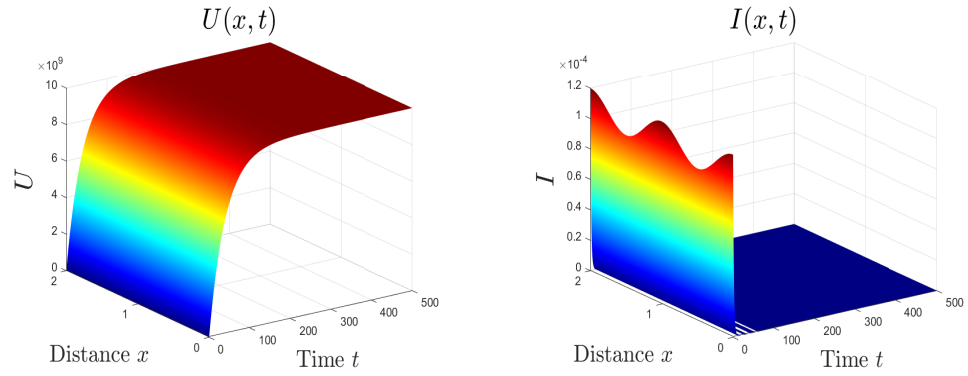

(**a**) Healthy RBCs

(**b**) Infected RBCs

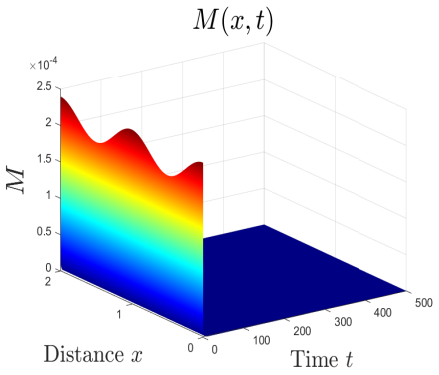

(**c**) Free merozoites

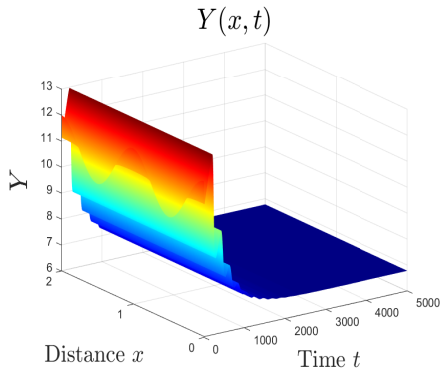

(**d**) Healthy ECs

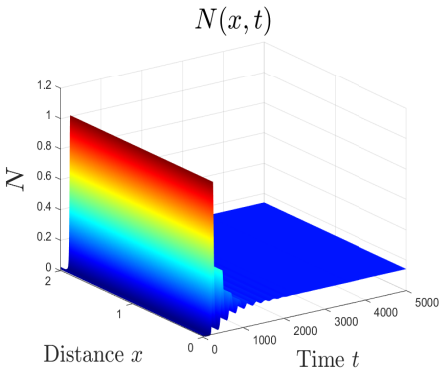

(**e**) Infected ECs

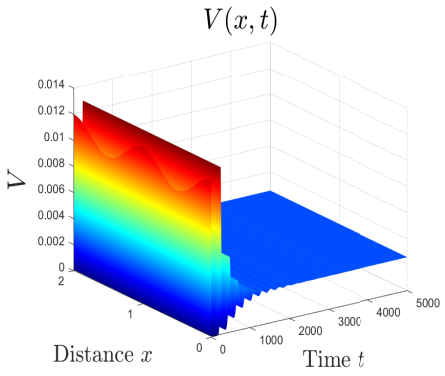

(**f**) Free SARS-CoV-2 particles

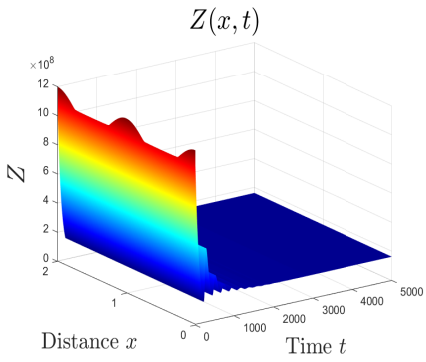

(**g**) Antibodies

Figure 5. Simulation of system (1) for $(\beta_m, \beta_v, p_1, p_2, d_7) = (2 \times 10^{-10}, 0.9, 3 \times 10^{-8}, 3.9, 0.01)$. The equilibrium $E_4 = (10 \times 10^9, 0, 0, 6.775, 0.1421, 0.0026, 1.628 \times 10^8)$ is GAS.

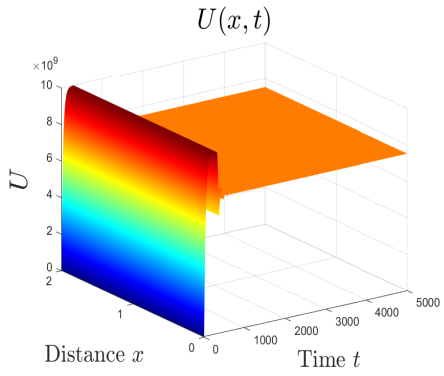

(**a**) Healthy RBCs

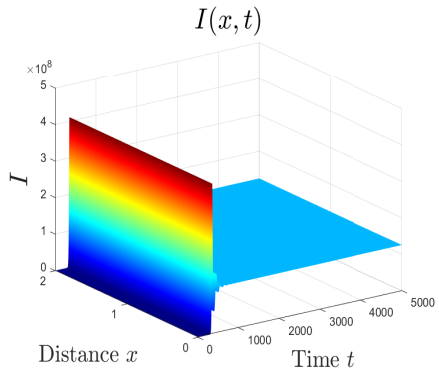

(**b**) Infected RBCs

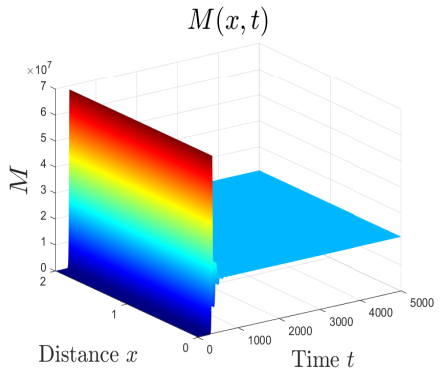

(**c**) Free merozoites

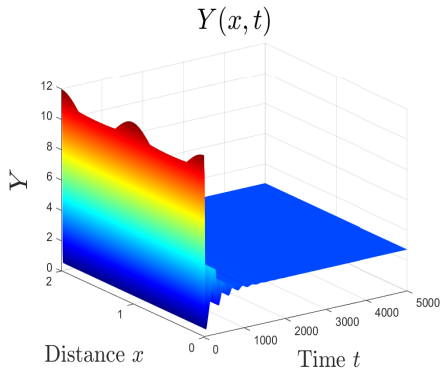

(**d**) Healthy ECs

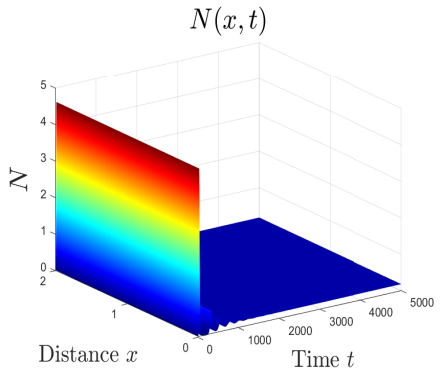

(**e**) Infected ECs

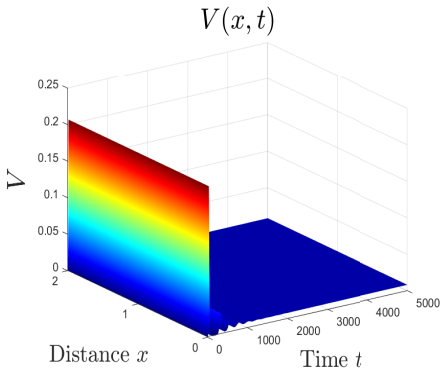

(**f**) Free SARS-CoV-2 particles

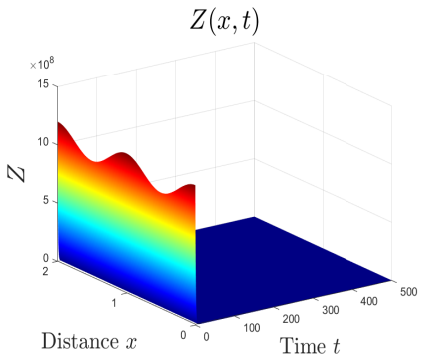

(**g**) Antibodies

Figure 6. Simulation of system (1) for $(\beta_m, \beta_v, p_1, p_2, d_7) = (4 \times 10^{-10}, 0.9, 3 \times 10^{-8}, 0.96, 0.8)$. The equilibrium $E_5 = (7.5 \times 10^9, 1.25 \times 10^8, 2.08 \times 10^7, 2.73, 0.1789, 0.008, 0)$ is GAS.

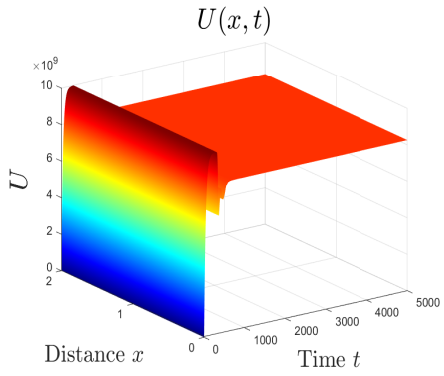

(**a**) Healthy RBCs

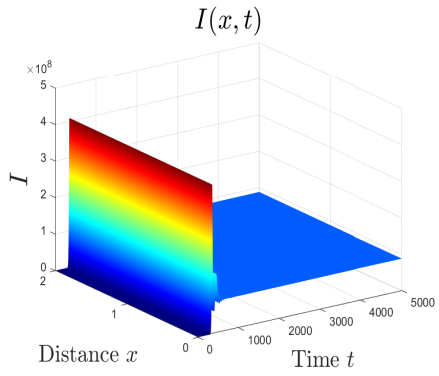

(**b**) Infected RBCs

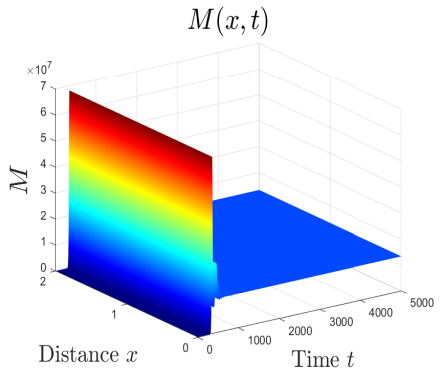

(**c**) Free merozoites

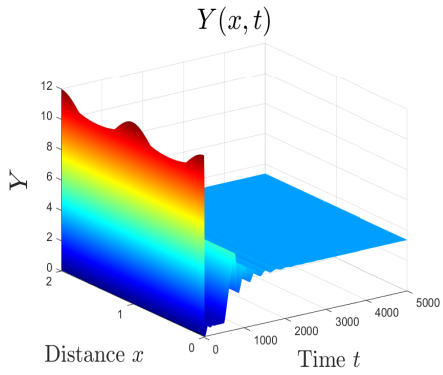

(**d**) Healthy ECs

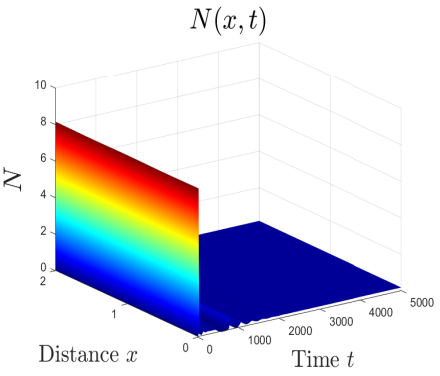

(**e**) Infected ECs

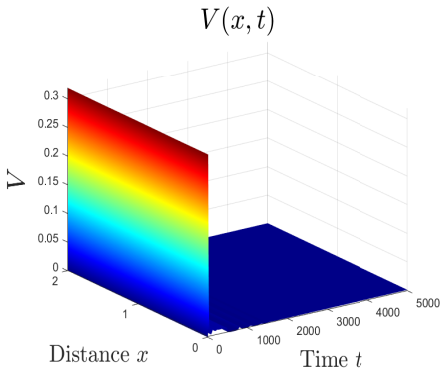

(**f**) Free SARS-CoV-2 particles

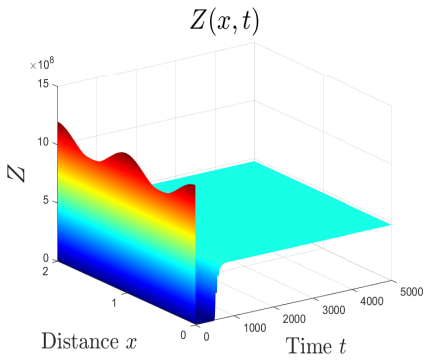

(**g**) Antibodies

Figure 7. Simulation of system (1) for $(\beta_m, \beta_v, p_1, p_2, d_7) = (4 \times 10^{-10}, 3.9, 3 \times 10^{-8}, 0.5, 0.4)$. The equilibrium $E_6 = (8.244 \times 10^9, 8.78 \times 10^7, 1.33 \times 10^7, 3.36, 0.17, 0.0015, 4.76 \times 10^8)$ is GAS.

5.1. Sensitivity Analysis

Sensitivity analysis evaluates a relative change in a variable when a parameter changes. We execute sensitivity analysis for $\mathcal{R}_{0m}$ and $\mathcal{R}_{0v}$ as they are the main determinants for the stability of the uninfected equilibrium E_0. The normalized forward sensitivity index of a differentiable function θ with respect to a parameter p is defined as

$$\Gamma_p^{\theta} = \frac{\partial \theta}{\partial p} \cdot \frac{p}{\theta}.$$

5.1.1. Sensitivity Analysis of $\mathcal{R}_{0m}$

The normalized forward sensitivity index of $\mathcal{R}_{0m}$ is given by

$$\Gamma_p^{\mathcal{R}_{0m}} = \frac{\partial \mathcal{R}_{0m}}{\partial p} \cdot \frac{p}{\mathcal{R}_{0m}}.$$

We calculate the sensitivity indices of $\mathcal{R}_{0m}$ with respect to each parameter using the values provided in Table 1. The results are listed in Table 2. We note that the sensitivity indices of $\mathcal{R}_{0m}$ do not depend on any parameters. For instance, the sensitivity index of $\mathcal{R}_{0m}$ with respect to η is

$$\Gamma_{\eta}^{\mathcal{R}_{0m}} = \frac{\partial \mathcal{R}_{0m}}{\partial \eta} \cdot \frac{\eta}{\mathcal{R}_{0m}} = \frac{\beta_m \sigma_1}{d_1 d_3} \cdot \frac{\eta d_1 d_3}{\eta \beta_m \sigma_1} = 1.$$

Therefore, it is useful to justify the sign of the sensitivity indices of $\mathcal{R}_{0m}$. According to Table 2, the number of merozoites produced per infected cell, η, the infection rate of RBCs, β_m, and the recruitment rate of healthy RBCs, σ_1, are the parameters that increase malaria infection in the body. Conversely, the death rate of uninfected RBCs, d_1, and the death rate of merozoites, d_3, are the parameters that have a crucial role in eliminating malaria infection from the body.

Table 2. Sensitivity indices of $\mathcal{R}_{0m}$.

Parameter	Sensitivity Index
η	1
β_m	1
σ_1	1
d_1	-1
d_3	-1

5.1.2. Sensitivity Analysis of $\mathcal{R}_{0v}$

The normalized forward sensitivity index of $\mathcal{R}_{0v}$ is given by

$$\Gamma_p^{\mathcal{R}_{0v}} = \frac{\partial \mathcal{R}_{0v}}{\partial p} \cdot \frac{p}{\mathcal{R}_{0v}}.$$

As for $\mathcal{R}_{0m}$, we calculate the sensitivity index of each parameter in $\mathcal{R}_{0v}$ using the values given in Table 1. The results are presented in Table 3. We see that, when one of the parameters with a positive index (e, β_v, or σ_2) is increased while the other parameters remain constant, this raises the value of $\mathcal{R}_{0v}$. In other words, these parameters lead to the growth of SARS-CoV-2. Conversely, the parameters with negative indices have a role in eliminating SARS-CoV-2 infection from the body.

Table 3. Sensitivity indices of $\mathcal{R}_{0v}$.

Parameter	Sensitivity Index
e	1
β_v	1
σ_2	1
d_4	-1
d_5	-1
d_6	-1

6. Results and Discussion

Malaria/COVID-19 coinfection represents a true concern especially in malaria-endemic regions. Therefore, there is an urgent need to understand the dynamics of this coinfection within a human body. In this paper, we develop a reaction–diffusion in-host malaria/COVID-19 coinfection model. This model considers the interactions between healthy RBCs, infected RBCs, free merozoites, healthy ECs, infected ECs, free SARS-CoV-2 particles and antibodies. We show that the system admits seven equilibrium points and we prove the following:

(1) The uninfected equilibrium E_0 always exists. Moreover, E_0 is GAS if $\mathcal{R}_{0m} \leq 1$ and $\mathcal{R}_{0v} \leq 1$. This situation represents an individual who recovered from both malaria and SARS-CoV-2 infections.

(2) The malaria single-infection without immunity equilibrium E_1 exists if $\mathcal{R}_{0m} > 1$. In addition, E_1 is GAS if $\mathcal{R}_{0v} \leq 1$ and $\mathcal{R}_{1m} \leq 1$. This simulates the situation of malaria mono-infection patient with inactive immunity.

(3) The malaria single-infection with immunity equilibrium E_2 exists if $\mathcal{R}_{1m} > 1$. Moreover, E_2 is GAS if $\mathcal{R}_p \leq 1 + \dfrac{\eta\beta_m\sigma_1 p_1 q_2}{q_1 d_6(p_1 d_1 + \beta_m d_7)}$. At this point, the antibody immune response is activated to eradicate malaria merozoites.

(4) The SARS-CoV-2 single-infection without immunity equilibrium E_3 exists if $\mathcal{R}_{0v} > 1$. In addition, E_3 is GAS if $\mathcal{R}_{0m} \leq 1$ and $\mathcal{R}_{1v} \leq 1$. This point simulates the situation of a patient who is only infected by SARS-CoV-2 and the immune response is inactive.

(5) The SARS-CoV-2 single-infection with immunity equilibrium E_4 exists if $\mathcal{R}_{1v} > 1$. It is GAS when $\mathcal{R}_{0m} + \dfrac{q_1 d_6}{q_2 d_3} \leq 1 + \dfrac{e\beta_v q_1 \sigma_2 p_2}{q_2 d_3 d_5(p_2 d_4 + \beta_v d_7)}$. The immune response is activated in the SARS-CoV-2 mono-infection patient.

(6) The malaria/COVID-19 coinfection without immunity equilibrium E_5 exists if $\mathcal{R}_{0m} > 1$ and $\mathcal{R}_{0v} > 1$. It is GAS when $\mathcal{R}_{0m} + \dfrac{e\beta_m\sigma_2 p_2}{p_1 d_1 d_5 d_6} \leq 1 + \dfrac{\beta_m(p_2 d_4 + \beta_v d_7)}{\beta_v p_1 d_1}$. Here, the coinfection occurs with inactive immune response.

(7) The malaria/COVID-19 coinfection with immunity equilibrium E_6 exists, and it is GAS if $\mathcal{R}_p > 1 + \dfrac{\eta\beta_m\sigma_1 p_1 q_2}{q_1 d_6(p_1 d_1 + \beta_m d_7)}$, $\mathcal{R}_{0m} + \dfrac{q_1 d_6}{q_2 d_3} > 1 + \dfrac{q_1 d_6}{q_2 d_3}\mathcal{R}_{1v}$, and $\mathcal{R}_{0m} + \dfrac{e\beta_m\sigma_2 p_2}{p_1 d_1 d_5 d_6} > 1 + \dfrac{\beta_m(p_2 d_4 + \beta_v d_7)}{\beta_v p_1 d_1}$. This point represents the occurrence of malaria/COVID-19 coinfection with an active antibody immune response.

The numerical results agree with the analytical results. Based on our results, we assume that the malaria/COVID-19 coinfection can be protective as the shared antibody immune response works on clearing SARS-CoV-2. This can decrease the severity of COVID-19. This result comes in agreement with some studies that reported the positive impact of the shared antibody immune response [4,17–19]. However, other studies suggested that there is an increased risk of death in malaria patients with SARS-CoV-2 infection [1,13]. Therefore, more studies are required to investigate the impact of coinfection between malaria and COVID-19, to evaluate the effect of the immune system during the coinfection, and to find the suitable ways for treating the coinfected patients. The main limitation of

this research work is that we did not estimate the values of the model's parameters using real data. The reasons are as follows: (1) The data on malaria/COVID-19 coinfection are still very limited; (2) Comparing our results with a small number of real studies may not be very precise; (3) Collecting real data from patient coinfected with malaria and SARS-CoV-2 is not an easy process; (4) Working on experiments to obtain data is beyond the scope of this paper. Thus, the theoretical results obtained in this paper need to be tested against empirical findings when real data become available.

6.1. Conclusions

Malaria/COVID-19 coinfection has been reported in many countries. In this paper, we formulated a reaction–diffusion in-host model to study the coinfection between malaria and COVID-19. We assumed that the shared antibody immune response decreases the concentrations of SARS-CoV-2 and malaria merozoites. This can reduce the severity of SARS-CoV-2 in coinfected patients. The principal limitation of this paper is that we did not use real data to estimate the values of parameters or to compare the results due to the scarcity of data. Therefore, our results need to be validated when real data become available.

6.2. Future Works

The model developed in this work can be improved by (i) using real data to find a good estimation of the parameters' values, (ii) examining the influence of time delays that may occur during infection or production of SARS-CoV-2 particles and malaria merozoites, (iii) considering viral mutations [41,50,51], (iv) considering the effect of treatments on the progression of both diseases, (v) incorporating the role of CTLs in killing infected RBCs or ECs, and (vi) considering an age-structured model to account for the age structure in the infected cells compartments, which can lead to important observations.

Supplementary Materials: The following supporting information can be downloaded at: https://www.mdpi.com/article/10.3390/math10224390/s1, File S1.

Author Contributions: Conceptualization, A.M.E. and A.D.A.A.; Formal analysis, A.M.E. and A.D.A.A.; Investigation, A.D.A.A.; Methodology, A.M.E. and A.D.A.A.; Writing—original draft, A.D.A.A.; Writing—review & editing, A.M.E. and A.D.A.A. All authors have read and agreed to the published version of the manuscript .

Funding: This research work was funded by Institutional Fund Projects under grant no. (IFPIP: 68-130-1443) provided by the Ministry of Education and King Abdulaziz University, DSR, Jeddah, Saudi Arabia.

Data Availability Statement: Not applicable.

Acknowledgments: This research work was funded by Institutional Fund Projects under Grant No. (IFPIP: 68-130-1443). The authors gratefully acknowledge technical and financial support provided by the Ministry of Education and King Abdulaziz University, DSR, Jeddah, Saudi Arabia.

Conflicts of Interest: The authors declare no conflict of interest.

References

1. Wilairatana, P.; Masangkay, F.; Kotepui, K.; Milanez, G.; Kotepui, M. Prevalence and characteristics of malaria among COVID-19 individuals: A systematic review, meta-analysis, and analysis of case reports. *PLoS Neglected Trop. Dis.* **2021**, *15*, e0009766. [CrossRef]
2. Akula, S.M.; Abrams, S.L.; Steelman, L.S.; Candido, S.; Libra, M.; Lerpiriyapong, K.; Cocco, L.; Ramazzotti, G.; Ratti, S.; Follo, M.Y.; et al. Cancer therapy and treatments during COVID-19 era. *Adv. Biol. Regul.* **2020**, *77*, 100739. [CrossRef]
3. Jyotsana, N.; King, M. The impact of COVID-19 on cancer risk and treatment. *Cell. Mol. Bioeng.* **2020**, *2016*, 5230219. [CrossRef]
4. Hussein, M.; Albashir, A.; Elawad, O.; Homeida, A. Malaria and COVID-19: Unmasking their ties. *Malar. J.* **2020**, *19*, 457. [CrossRef]
5. Di Gennaro, F.; Marotta, C.; Locantore, P.; Pizzol, D.; Putoto, G. Malaria and COVID-19: Common and different findings. *Trop. Med. Infect. Dis.* **2020**, *5*, 141. [CrossRef]

6. Coronavirus Disease (COVID-19), Vaccine Tracker, World Health Organization (WHO). 2021. Available online: https://covid19.trackvaccines.org/agency/who/ (accessed on 1 October 2022).
7. The U.S. Food and Drug Administration. Know Your Treatment Options for COVID-19. 2021. Available online: https://www.fda.gov/consumers/consumer-updates/know-your-treatment-options-covid-19 (accessed on 1 November 2022).
8. Elaiw, A.M.; Al Agha, A.D. Global analysis of a reaction–diffusion within-host malaria infection model with adaptive immune response. *Mathematics* **2020**, *8*, 563. [CrossRef]
9. Malaria, Fact Sheets, World Health Organization (WHO). 2021. Available online: https://www.who.int/news-room/fact-sheets/detail/malaria (accessed on 1 October 2022).
10. Sebastiao, C.; Gaston, C.; Paixao, J.; Sacomboio, E.; Neto, Z.; de Vasconcelos, J.N.; Morais, J. Coinfection between SARS-CoV-2 and vector-borne diseases in Luanda, Angola. *J. Med. Virol.* **2021**, *94*, 366–371. [CrossRef]
11. Pusparani, A.; Henrina, J.; Cahyadi, A. Co-infection of COVID-19 and recurrent malaria. *J. Infect. Dev. Ctries.* **2021**, *15*, 625–629. [CrossRef]
12. Chanda-Kapata, P.; Kapata, N.; Zumla, A. COVID-19 and malaria: A symptom screening challenge for malaria endemic countries. *Int. J. Infect. Dis.* **2020**, *94*, 151–153. [CrossRef]
13. Indari, O.; Baral, B.; Muduli, K.; Mohanty A.; Swain, N.; Mohakud, N.K.; Jha, H.C. Insights into Plasmodium and SARS-CoV-2 co-infection driven neurological manifestations. *Biosaf. Health* **2021**, *3*, 230–234. [CrossRef]
14. Mahajan, N.N.; Kesarwani, S.N.; Shinde, S.S.; Nayak, A.; Modi, D.N.; Mahale, S.D.; Gajbhiye, R.K. Co-infection of malaria and dengue in pregnant women with SARS-CoV-2. *Int. J. Gynecol. Obstet.* **2020**, *151*, 459–462. [CrossRef]
15. Hussein, R.; Guedes, M.; Ibraheim, N.; Ali, M.M.; El-Tahir, A.; Allam, N.; Abuakar, H.; Pecoits-Filho, R.; Kotanko, P. Co-infection of malaria and early clearance of SARS-CoV-2 in healthcare workers. *J. Med. Virol.* **2021**, *93*, 2431–2438.
16. Hussein, R.; Guedes, M.; Ibraheim, N.; Ali, M.M.; El-Tahir, A.; Allam, N.; Abuakar, H.; Pecoits-Filho, R.; Kotanko, P. Impact of COVID-19 and malaria coinfection on clinical outcomes: A retrospective cohort study. *Clin. Microbiol. Infect.* **2022**, *28*, 1152.e1–1152.e6. [CrossRef]
17. Kalungi, A.; Kinyanda, E.; Akena, D.; Kaleebu, P.; Bisangwa, I. Less Severe Cases of COVID-19 in Sub-Saharan Africa: Could Co-infection or a Recent History of Plasmodium falciparum Infection Be Protective? *Front. Immunol.* **2021**, *12*, 565625. [CrossRef]
18. Parodi, A.; Cozzani, E.Coronavirus disease 2019 (COVID 19) and Malaria. *Med. Hypotheses* **2020**, *143*, 110036. [CrossRef]
19. Iesa, M.; Osman, M.; Hassan, M.; Dirar, A.; Abuzeid, N.; Mancuso, J.J.; Pandey, R.; Mohammed, A.A.; Borad, M.J.; Babiker, H.M. SARS-CoV-2 and Plasmodium falciparum common immunodominant regions may explain low COVID-19 incidence in the malaria-endemic belt. *New Microbes New Infect.* **2020**, *38*, 100817. [CrossRef]
20. Anderson, R.; May, R.; Gupta, S. Nonlinear phenomena in host-parasite interactions. *Parasitology* **1989**, *99*, S59–S79. [CrossRef]
21. Hetzel, C.; Anderson, R. The within-host cellular dynamics of bloodstage malaria: Theoretical and experimental studies. *Parasitology* **1996**, *113*, 25–38. [CrossRef]
22. Saul, A. Models for the in-host dynamics of malaria revisited: Errors in some basic models lead to large over-estimates of growth rates. *Parasitology* **1998**, *117*, 405–407. [CrossRef]
23. Hoshen, M.; Heinrich, R.; Stein, W.; Ginsburg, H. Mathematical modelling of the within-host dynamics of Plasmodium falciparum. *Parasitology* **2000**, *121*, 227–235. [CrossRef]
24. Iggidr, A.; Kamgang, J.; Sallet, G.; Tewa, J. Global analysis of new malaria intrahost models with a competitive exclusion principle. *SIAM J. Appl. Math.* **2006**, *67*, 260–278. [CrossRef]
25. Tumwiine, J.; Mugisha, J.; Luboobi, L. On global stability of the intra-host dynamics of malaria and the immune system. *J. Math. Anal. Appl.* **2008**, *341*, 855–869. [CrossRef]
26. Orwa, T.; Mbogo, R.; Luboobi, L. Mathematical model for the in-host malaria dynamics subject to malaria vaccines. *Lett. Biomath.* **2018**, *5*, 222–251. [CrossRef]
27. Asamoah, J.; Jin, Z.; Sun, G.; Seidu, B. Sensitivity assessment and optimal economic evaluation of a new COVID-19 compartmental epidemic model with control interventions. *Chaos Soiltons Fractals* **2021**, *146*, 110885. [CrossRef]
28. Currie, C.; Fowler, J.; Kotiadis, K.; Monks, T. How simulation modelling can help reduce the impact of COVID-19. *J. Simul.* **2020**, *14*, 83–97. [CrossRef]
29. Krishna, M.V.; Prakash, J. Mathematical modelling on phase based transmissibility of Coronavirus. *Infect. Dis. Model.* **2020**, *5*, 375–385. [CrossRef]
30. Rajagopal, K; Hasanzadeh, N.; Parastesh, F.; Hamarash, I.; Jafari, S.; Hussain, I. A fractional-order model for the novel coronavirus (COVID-19) outbreak. *Nonlinear Dyn.* **2020**, *101*, 711–718. [CrossRef]
31. Chen, T.; Rui, J.; Wang, Q.; Zhao, Z.; Cui, J.A.; Yin, L. A mathematical model for simulating the phase-based transmissibility of a novel coronavirus. *Infect. Dis. Poverty* **2020**, *9*, 24. [CrossRef]
32. Liu, Z.; Magal, P.; Seydi, O.; Webb, G. Understanding unreported cases in the 2019-nCoV epidemic outbreak in Wuhan, China, and the importance of major public health interventions. *SSRN Electronic J.* **2020**, 1–12. [CrossRef]
33. Du, S.Q.; Yuan, W. Mathematical modeling of interaction between innate and adaptive immune responses in COVID-19 and implications for viral pathogenesis. *J. Med. Virol.* **2020**, *92*, 1615–1628. [CrossRef]
34. Li, C.; Xu, J.; Liu, J.; Zhou, Y. The within-host viral kinetics of SARS-CoV-2. *Math. Biosci. Eng.* **2020**, *17*, 2853–2861. [CrossRef]
35. Ghosh, I. Within host dynamics of SARS-CoV-2 in humans: Modeling immune responses and antiviral treatments. *arXiv* **2020**, arXiv:2006.02936.

36. Pinky, L.; Dobrovolny, H.M. SARS-CoV-2 coinfections: Could influenza and the common cold be beneficial?. *J. Med. Virol.* **2020**, *92*, 2623–2630. [CrossRef]
37. Elaiw, A.M.; Al Agha, A.D.; Azoz, S.A.; Ramadan, E. Global analysis of within-host SARS-CoV-2/HIV coinfection model with latency. *Eur. Phys. J. Plus* **2022**, *137*, 1–22. [CrossRef]
38. Elaiw, A.M.; Al Agha, A.D. Global dynamics of SARS-CoV-2/cancer model with immune responses. *Appl. Math. Comput.* **2021**, *408*, 126364. [CrossRef]
39. Al Agha, A.D.; Elaiw, A.M. Global dynamics of SARS-CoV-2/malaria model with antibody immune response. *Math. Eng.* **2022**, *19*, 8380–8410. [CrossRef]
40. Takoutsing, E.; Temgoua, A.; Yemele, D.; Bowong, S. Dynamics of an intra-host model of malaria with periodic antimalarial treatment. *Int. J. Nonlinear Sci.* **2019**, *27*, 148–164.
41. Elaiw, A.M.; Al Agha, A.D.; Alshaikh, M.A. Global stability of a within-host SARS-CoV-2/cancer model with immunity and diffusion. *Int. J. Biomath.* **2022**, *15*, 2150093. [CrossRef]
42. Zhang, Y.; Xu, Z.Dynamics of a diffusive HBV model with delayed Beddington-DeAngelis response. *Nonlinear Anal. Real World Appl.* **2014**, *15*, 118–139. [CrossRef]
43. Xu, Z.; Xu, Y. Stability of a $CD4^+$ T cell viral infection model with diffusion. *Int. J. Biomath.* **2018**, *11*, 1850071. [CrossRef]
44. Smith, H.L. *Monotone Dynamical Systems: An Introduction to the Theory of Competitive and Cooperative Systems*; American Mathematical Society: Providence, RI, USA, 1995.
45. Protter, M.H., Weinberger, H.F. *Maximum Principles in Differential Equations*; Prentic Hall: Englewood Cliffs, NJ, USA, 1967.
46. Henry, D. *Geometric Theory of Semilinear Parabolic Equations*; Springer: New York, NY, USA, 1993.
47. Khalil, H.K. *Nonlinear Systems*; Prentice-Hall: Englewood Cliffs, NJ, USA, 1996.
48. Elaiw, A.; Al Agha, A. Global dynamics of reaction–diffusion oncolytic M1 virotherapy with immune response. *Appl. Math. Comput.* **2020**, *367*, 124758. [CrossRef]
49. Almocera, A.S.; Quiroz, G.; Hernandez-Vargas, E.A. Stability analysis in COVID-19 within-host model with immune response. *Commun. Nonlinear Sci. Numer. Simul.* **2020**, *95*, 105584. [CrossRef]
50. Bellomo, N.; Burini, D.; Outada, N. Multiscale models of Covid-19 with mutations and variants. *Netw. Heterog. Media* **2022**, *17*, 293–310. [CrossRef]
51. Bellomo, N.; Burini, D.; Outada, N. Pandemics of mutating virus and society: A multi-scale active particles approach. *Philos. Trans. A Math. Phys. Eng. Sci.* **2022**, *380*, 20210161. [CrossRef]